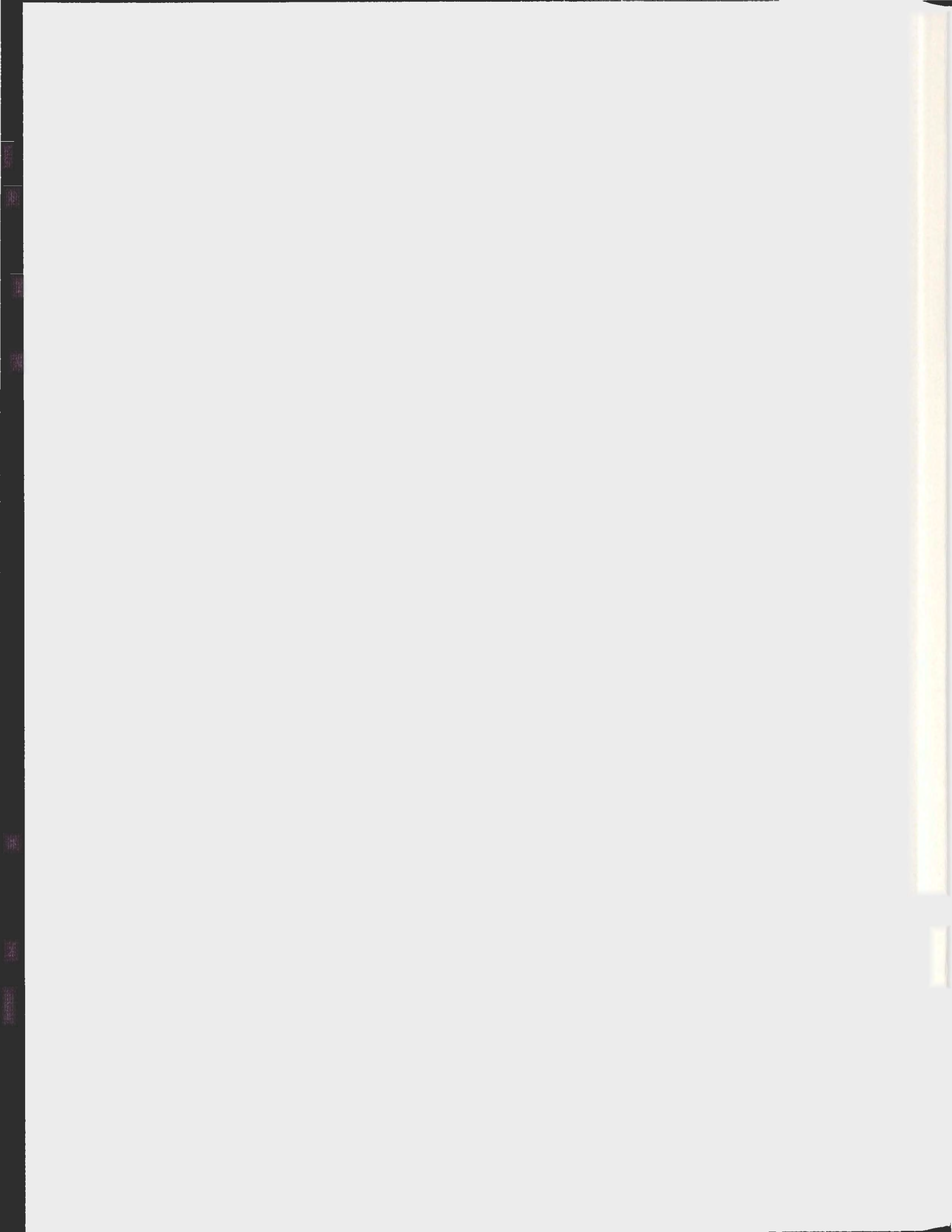


EFFECTS OF CHRONIC SUBCUTANEOUS ADMINISTERED
PROTEINASE-ACTIVATED RECEPTOR 2-ACTIVATING
PEPTIDE ON VASCULAR REACTIVITY OF AORTAS
AND BLOOD PRESSURES IN MICE

KEON H. HUGHES



Effects of chronic subcutaneous administered proteinase-activated receptor 2-activating peptide on vascular reactivity of aortas and blood pressures in mice.

By

© Keon H. Hughes

A thesis submitted to the School of Graduate Studies

in partial fulfilment of the

requirements for the degree of

Master of Science (Medicine)

Cardiovascular and Renal Sciences

Memorial University

October 2011

St. John's

Newfoundland and Labrador

Abstract

The acute *in vivo* effects of proteinase-activated receptor 2 activating peptides (PAR₂-AP) are reported to include vascular inflammation and hypotension. We studied the time- (7 and 14 days) and dose-dependent (2 nmol/kg/min and 6 nmol/kg/min) effects of chronic subcutaneous infusion with a PAR₂-AP, 2-furoyl-LIGRLO-NH₂ (2fly), in C57BL/6J (C57) mice and PAR₂-deficient (PAR₂^{-/-}) mice. In aortas from PAR₂-AP treated C57 mice the relaxation curve generated by 2fly was rightwardly shifted relative to saline-treated C57 mice. At specific times and doses of PAR₂-AP treatment in C57 mice, the maximal endothelium-dependent (acetylcholine) and -independent (nitroprusside) nitric oxide-mediated relaxations of aortas were less than in saline-treated C57. Aortic expression of proteins associated with PAR₂-AP induced smooth muscle relaxation was not significantly different between mouse strains and treatment groups. In C57 mice, 24 h hemodynamics and locomotor activity measured by radiotelemetry throughout the infusion periods indicated that 2fly high dose treatment lowered arterial systolic and pulse pressures relative to the baseline period when compared to saline infusions. We conclude that PAR₂-AP administered chronically *in vivo* produced aortic dysfunction in C57 mice which was characterized by attenuated endothelium-dependent PAR₂, cholinergic, and endothelium-independent nitric oxide-mediated relaxations. In spite of the *in vivo* vascular dysfunction, high dose 2fly-treatment lowered the systolic and pulse blood pressures of C57 mice.

Acknowledgements

First off I would like to thank my supervisor Dr. John McGuire for providing me the guidance and leadership needed to complete this thesis. His supervision has helped me understand the research process, from hypothesis forming, to writing of scientific papers, and questioning the validity of hypotheses put forth by me or others.

Secondly, I would like to thank the faculty and staff of the Cardiovascular and Renal Sciences Group of Memorial University. I would like to thank Dr. John Smeda and Dr. Bruno Stuyvers for their help during development of different stages of my experiments as well as providing great advice. I would also like to thank Dr. Bruce Van Vliet for guidance on telemetry. Many others have helped me in many ways throughout my thesis. Sarah Halfyard, Elizabeth Chia, Dr. Enoka Wijekoon, Dr. Satomi Kagota, and Dr. Noriko Daneshtalab have all helped me learn different techniques while providing a friendly and enjoyable environment in which to work. Finally, I am thankful for encouragement and support from Santana and my parents. Without their help completion of my thesis would have not been possible.

Funding for the research described within this thesis was made possible through grants from the Government of Newfoundland and Labrador (Industrial Research and Innovation Fund) and the Canadian Institutes of Health Research (Regional Partnership Program) awarded to Dr. John McGuire.

Table of Contents

Abstract	i
Acknowledgements	ii
Co-Authorship.....	v
List of Tables	vi
List of Figures	vii
List of Abbreviations	ix
List of Appendices	xi
Chapter 1: Introduction	1
1.1 Research problem	1
1.2 Rationale.....	2
1.3 Hypotheses and Objectives	5
Chapter 2: Literature Review	8
2.1 Proteinase-activated receptors (PARs).....	8
2.2 PAR ₂ -activating peptides	10
2.3 Cardiovascular actions of PAR ₂ -APs	11
2.4 <i>In vivo</i> effects of PAR ₂ -AP link with inflammation and immunity	13
2.5 PAR ₂ antagonists.....	15
2.6 PAR ₂ knockout mice	17
2.7 Endothelium-dependent relaxation mechanisms.....	19
2.8 Endothelium-independent nitrovasodilators	22
2.9 Non-hemodynamic effects of PAR ₂ -AP on endothelial cells.....	22
2.10 Methods for assessment of endothelial dysfunction.....	23
Chapter 3: Materials and Methods	25
3.1 Animal Ethics	25
3.2 Materials.....	25
3.3 Mice.....	26
3.4 Breeding Protocol.....	26
3.5 Genotyping	27
3.6 Radiotelemetry	29
3.7 Blood pressure and activity data analyses	30
	iii

3.8 Subcutaneous drug delivery	31
3.9 Isometric tension measurements of mouse aortas	32
3.10 Western Blots	34
3.11 Immunohistochemistry	36
3.12 Statistical Analyses.....	37
Chapter 4: Results	38
4.1 Effect of chronic PAR ₂ activation on NO-mediated relaxation of aortas	38
4.1.1 2fly Relaxation.....	38
4.1.2 Acetylcholine Relaxation.....	42
4.1.3 Nitroprusside Relaxation	46
4.1.4 A23187 Relaxation	46
4.1.5 Intact versus denuded endothelium.....	51
4.1.6 Effect of eNOS and COX inhibition on vasodilators.....	51
4.2 Chronic PAR ₂ -AP treatment effect on expressions of COX isoforms 1 and 2, eNOS and sGC in mouse aortas.....	55
4.3 Characteristics of SAM11 “anti-PAR ₂ ” antibody immunofluorescence in mouse aortas	58
4.4 Blood pressure, heart rate and locomotor activity.....	61
Chapter 5: Discussion	66
5.1 General Findings	66
5.2 Effects of administering chronic s.c. PAR ₂ -AP on mouse aortas <i>in vitro</i>	68
5.3 Effect of administering chronic s.c. PAR ₂ -AP on hemodynamics <i>in vivo</i>	70
5.4 Limitations to interpretations	71
5.5 Conclusions	72
References.....	73
Appendices.....	83

Co-Authorship

This thesis was based on research completed under the primary supervision of Dr. John McGuire and thesis supervisory committee members Dr. John Smeda and Dr. Bruno Stuyvers of the Cardiovascular-Renal Sciences Graduate Studies Program. Supervisors provided assistance with the research proposal, experimental design, and preparation of written work contained within.

List of Tables

Table 2.1 Tethered ligand sequences from human, rat, and mouse for each member of the PAR family.....	9
Table 2.2 PAR-activating peptides.....	11
Table 4.1. Parameters for 2fly CRC in saline and 2fly treated mice in the presence of nonselective inhibitors of NOS and COX.....	41
Table 4.2. Parameters for acetylcholine CRC in saline and 2fly treated C57 mice in the presence of nonselective inhibitors of NOS and COX.....	44
Table 4.3. Parameters for acetylcholine CRC in saline and 2fly treated PAR ₂ ^{-/-} mice in the presence of nonselective inhibitors of NOS and COX.....	45
Table 4.4. Parameters for nitroprusside CRC in saline and 2fly treated C57 mice in the presence of nonselective inhibitors of NOS and COX.....	48
Table 4.5. Parameters for nitroprusside CRC in saline and 2fly treated PAR ₂ ^{-/-} mice in the presence of nonselective inhibitors of NOS and COX.....	49
Table 4.6. 24 h baseline hemodynamics and locomotor activity data from C57 and PAR ₂ ^{-/-} mice.....	63

List of Figures

Figure 1.1 Experimental design for mice treatment.....	6
Figure 2.1 Illustration comparing PAR ₂ activation by enzymes versus PAR ₂ -AP.....	10
Figure 2.2 Vascular smooth muscle relaxation by PAR ₂ activation via endothelial-derived NO.....	22
Figure 4.1. Effect of PAR ₂ -AP s.c. infusions for 7 (A) and 14 (B) days on 2fly-induced relaxations of isolated C57 aortas.....	39
Figure 4.2. Effect of PAR ₂ -AP s.c. infusions for 7 (A, C) and 14 (B, D) days on acetylcholine-induced relaxations of isolated C57 aortas PAR ₂ ^{-/-} aortas.....	43
Figure 4.3. Effect of PAR ₂ -AP s.c. infusions for 7 (A, C) and 14 (B, D) 14 days on nitroprusside-induced relaxations of isolated C57 and PAR ₂ ^{-/-} aortas.....	47
Figure 4.4. Effect of PAR ₂ -AP s.c. infusions for 7 (A, C) and 14 (B, D) days on A23187-induced relaxations of isolated C57 and PAR ₂ ^{-/-} aortas.....	50
Figure 4.5. Effect of endothelium denudation of C57 aortas on 2fly-, acetylcholine-, nitroprusside- and A23187-induced relaxations.....	52
Figure 4.6. Effect of endothelium denudation of PAR ₂ ^{-/-} aortas on acetylcholine-, nitroprusside- and A23187-induced relaxations.....	53
Figure 4.7. Effect of indomethacin on 2fly-induced relaxations of aortas from PAR ₂ -AP treated C57.....	54

Figure 4.8. Expression of COX-1 and COX-2 proteins in aortas of C57 mice infused s.c. with saline or high dose 2fly for 14 days.....	56
Figure 4.9. Expression of sGC and eNOS protein in aortas of C57 and PAR ₂ ^{-/-} mice infused s.c. with saline or low dose 2fly for 14 days.....	57
Figure 4.10. Immunofluorescence of PAR ₂ in aortas of C57 mice.....	59
Figure 4.11. Immunofluorescence of PAR ₂ in aortas of PAR ₂ ^{-/-} mice.....	60
Figure 4.12. Mean 24 h hemodynamics and locomotor activity in C57 and PAR ₂ ^{-/-} during a 4 day baseline period and 14 days treatment with high dose s.c. administered 2fly.....	64
Figure 4.13. Changes in 24 h mean hemodynamic and locomotor activities relative to baseline for C57 and PAR ₂ ^{-/-} during 14 day treatments with high dose s.c. administered 2fly	65

List of Abbreviations

- 2fly – 2-furoyl-LIGRLO-NH₂
- A23187 – calcium ionophore
- ACh – acetylcholine
- BP – blood pressure
- C57– C57BL/6J mice
- cGMP – 3, 5 cyclic guanosine monophosphate
- COX-*n* – cyclooxygenase-*n*, where *n* = 1 or 2
- CRC – concentration response curve
- DNA – deoxyribonucleic acid
- ENMD-1068 – *N*1-3-methylbutyryl-*N*4-6-aminohexanoyl-piperazine
- eNOS – endothelial nitric oxide synthase
- FITC – fluorescein isothiocyanate
- GTP – guanosine triphosphate
- i.v. – intravenous
- IL-*n* – interleukin, where *n*= the interleukin number
- L-NAME – *N*ω-nitro-L-arginine-methyl ester
- M3 – type 3 muscarinic receptor
- NO – nitric oxide
- PAR_{*n*} – proteinase-activated receptor *n*, where *n*=1, 2, 3 or 4; also known as protease-activated receptors

PAR₂ – also known as factor 2 receptor like 1 (*F2rl1*); GPCR-11

PAR₂^{-/-} – proteinase-activated receptor 2 knockout mice (B6.Cg-*F2rl1*^{tm1Mslb}/J)

PAR-AP – PAR-activating peptide

s.c. – subcutaneous

sGC – soluble guanylyl cyclase

U46619 – 9, 11-dideoxy-11 α , 9 α -epoxymethanoprostaglandin F_{2 α}

List of Appendices

Appendix A. Oligonucleotide primer sets for genotyping PAR ₂ ^{-/-} mice.....	82
Appendix B. Antibodies used in western blot analysis.....	83

Chapter 1: Introduction

1.1 Research problem

Cardiovascular diseases including myocardial infarction, stroke, and ischemic heart disease, accounted for 30% of all deaths in Canada during the years 2000 to 2006 (Statistics Canada, 2010). Hypertension is a major risk factor for these diseases and is one of the most common chronic clinical pathologies in Canadians. Hypertension has many underlying causes. A well known cause is increased peripheral vascular resistance to blood flow; this has been in part attributed to increased level of endothelium-derived contracting factors and decreased levels of endothelium-derived relaxing factors (Harrison, 1997). The constant imbalance of vasoactive substances in a blood vessel such that there is greater amounts of vasoconstrictive compared to vasorelaxant effects resulting in elevated blood pressure (BP) is one definition that is used to describe endothelial dysfunction. Increased blood pressure may lead to vascular damage (damage to the membrane integrity of the endothelium), which can be followed by inflammatory processes leading to atherosclerosis (Deanfield *et al.*, 2005). Endothelial dysfunction is associated with hypercholesterolemia, type 2 diabetes, and chronic inflammation (Brunner *et al.*, 2005). The interactions of endothelial dysfunction with multiple diseases makes this topic an area of research that needs to be further studied. It is possible that an intervention or functional offset of endothelial dysfunction may be a therapeutic benefit in cardiovascular diseases.

One possible target for intervention of endothelial dysfunction is PAR₂. In many studies, when this receptor was activated acutely it decreased inflammation pathologies (Kelso *et al.*, 2006, Lindner *et al.*, 2000; Schmidlin *et al.*, 2002; Robin *et al.*, 2003; Seeliger *et al.*, 2003) and lowered blood pressure (Cheung *et al.*, 1998; Damiano *et al.*, 1999; Wang *et al.*, 2010). A study of chronic activation of PAR₂ would add to the knowledge on how the body may function under the influence of a receptor system with capability for modulating both inflammation and vasorelaxation.

1.2 Rationale

Endothelial dysfunction has been described in animal models of chronic inflammation (Urbich and Dimmeler, 2004) and cardiovascular diseases (Anderson *et al.*, 1995; Panza *et al.*, 1990; Quyyumi *et al.*, 1997; Schachinger and Zeiher, 1995; Volpe *et al.*, 1996). During tissue inflammation or injury, the production of cytokines including interleukin-1 (IL-1 β) and interleukin-6 (IL-6) have been reported to contribute to the development of endothelium dysfunction. This dysfunction results in a diminished ability of vessels to modulate tone in response to either endogenous or exogenous vasoactive substances, such as bradykinin and acetylcholine. Endothelial dysfunction is associated with progression of cardiovascular diseases such as hypertension, cerebrovascular diseases, and coronary artery disease (Brunner *et al.*, 2005). Mediators of inflammation, which includes IL-1 β , have also been found to upregulate endothelial cell responses to proteinase-activated receptor 2 (PAR₂) activation (Nystedt *et al.*, 1996). For example PAR₂ activation by PAR₂-activating peptides (PAR₂-AP) can induce further cytokine (IL-

6, IL-8) production (Lourbakos *et al.*, 2001) and adhesion molecule expression in endothelial cells (Buddenkotte *et al.*, 2005; Shpacovitch *et al.*, 2004). If activating PAR₂ induces the production of cytokines then PAR₂ activation is expected to lead to endothelial dysfunction.

In vivo studies have reported that PAR₂-APs administered acutely causes a range of effects including hyperalgesia (Vergnolle *et al.*, 2001), increased salivary secretion (Kawabata *et al.*, 2000; Kawabata *et al.*, 2004), and scratching (Shimada *et al.*, 2006), which are effects that would be attributed to localized tissue inflammation. High doses of some PAR₂-APs have been found to generate non-PAR₂ vascular actions *in vitro*, and thus, provide potential confounding interpretations for *in vivo* studies (McGuire *et al.*, 2002a). In isolated blood vessel assays, nanomolar concentrations of PAR₂-APs cause vasodilation which is dependent on an intact endothelium and PAR₂ expression (McGuire *et al.*, 2002a; McGuire *et al.*, 2002b; Saifeddine *et al.*, 1996). The PAR₂-AP 2-furoyl-LIGRLO-NH₂ (2fly) has 30- to 100-times the *in vitro* potency of legacy PAR₂-APs (SLIGRL-NH₂) and lacks the non-PAR₂ effects of these compounds in the same assays (McGuire *et al.*, 2004a). Acutely administered intravenous (i.v.) PAR₂-APs, including 2fly, lowered blood pressures of anaesthetized rodents (Cheung *et al.*, 1998; Damiano *et al.*, 1999; Wang *et al.*, 2010). Decreases in mean arterial blood pressures in response to i.v. 2fly have been replicated in anaesthetized rats by our laboratory (McGuire and Tabrizchi, unpublished data). Acute PAR₂ infusions in humans caused an increase in forearm blood flow and were well-tolerated (Robin *et al.*, 2003). Interestingly, the

vasodilator effects of 2fly and other PAR₂-APs have been found to persist in resistance arteries under conditions when other endothelium-dependent relaxing agents have reduced efficacy (Kagota *et al.*, 2011; McGuire *et al.*, 2007; Smeda and McGuire, 2007; Smeda *et al.*, 2010). *In vitro* studies have reported a protective role of PAR₂ activation against ischemic reperfusion damage in the coronary vasculature (Napoli *et al.*, 2000). These effects appear to contradict the notion of PAR₂ activation causing endothelial dysfunction. In fact, protection against ischemia, persistent vasodilator activity, and blood pressure lowering effects of PAR₂-AP would suggest evidence of PAR₂-AP being useful against the negative effects of endothelial dysfunction.

Which way, agonist or antagonist, should we target PAR₂ to produce a therapeutic benefit? Acutely administered small molecule antagonists of PAR₂ have been reported to be effective in rodent models of acute inflammatory diseases, including the use ENMD-1068 in an immune system-induced arthritis model (Kelso *et al.*, 2006). Studies in PAR₂ gene knockout mice (PAR₂^{-/-}) indicate gene deficiency for this receptor is protective against several types of tissue inflammation including airway inflammation (Schmidlin *et al.*, 2002), contact dermatitis (Seeliger *et al.*, 2003), and colitis (Lindner *et al.*, 2000). However, there is also evidence to indicate that injury and inflammation responses were increased in PAR₂^{-/-}. Increased inflammation was found in mouse pancreatitis (Sharma *et al.*, 2005). Acute focal ischemic brain injury was reported to be higher in PAR₂^{-/-} (Jin *et al.*, 2005). In conscious unrestrained PAR₂^{-/-}, we reported significantly elevated systolic arterial and pulse pressures compared to their control strain

under baseline conditions (McGuire *et al.*, 2008). Our data were acquired by radiotelemetry, which is the method with the highest resolution for conscious blood pressure measurements. Other earlier studies, that collected hemodynamic data via carotid dwelling catheters in isoflurane-anaesthetized mice, reported no difference between PAR₂^{-/-} and control mice (Damiano *et al.*, 1999). A search of the most recent literature (to June 2011) indicates no published studies of the chronic effects of PAR₂-AP administered *in vivo*.

PAR₂ activation *in vivo* may be expected to induce inflammation leading to endothelium dysfunction, and thus, contribute to the development of cardiovascular diseases including hypertension. However, this possible effect does not exclude a time- or dose-dependent hypotensive effect of chronic administered PAR₂-AP.

1.3 Hypotheses and Objectives

This thesis tested two hypotheses. **Hypothesis 1** was that chronic treatment of mice with PAR₂-AP would induce time- and dose-dependent endothelium dysfunction linked to loss of endothelium-derived NO relaxation; PAR₂-AP would not cause endothelial dysfunction in PAR₂^{-/-}. **Hypothesis 2** was that chronic treatment of mice with PAR₂-AP would induce time-dependent lowering of blood pressures in normal mice with no effect in PAR₂^{-/-}.

To test **Hypothesis 1**, we established a chronic PAR₂-AP treatment model which comprised administering either of two doses of PAR₂-AP 2fly (2 nmol/kg/min (low dose, LD) and 6 nmol/kg/min (high dose, HD)) to normal healthy mice (C57BL/6J; C57) and

PAR₂-deficient (B6.Cg-F2r11^{tm1Mslb}/J; PAR₂^{-/-}) for 7 and 14 days by subcutaneous infusions via micro-osmotic pumps (Figure 1.1).

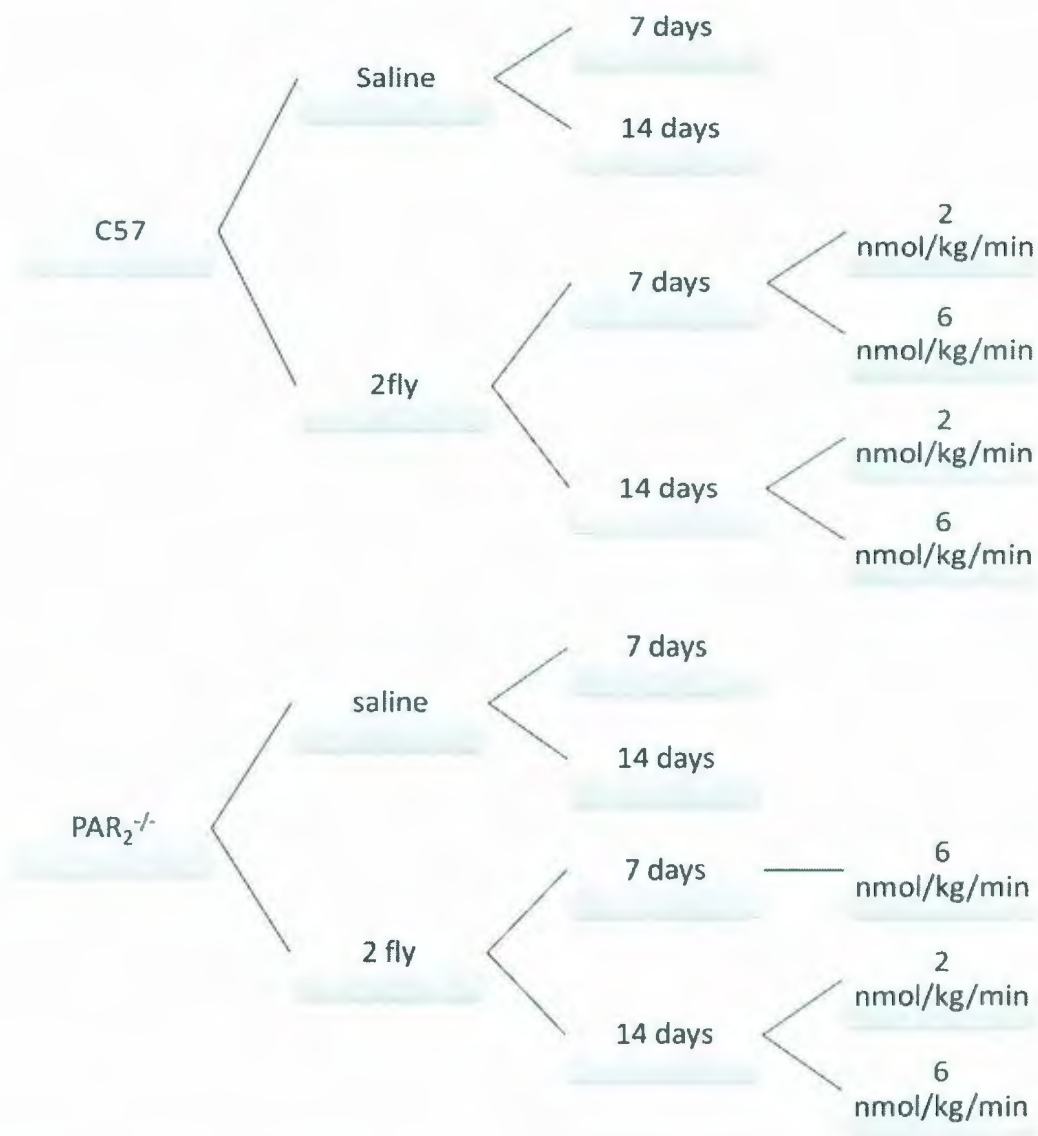


Figure 1.1 Experimental design for mice treatment. Abbreviations: C57, C57BL/6J mice; PAR₂^{-/-}, B6.Cg-F2r11^{tm1Mslb}/J mice; 2fly, 2-furoyl-LIGRLO-NH₂; saline, 0.9% NaCl; 2 nmol/kg/min, low dose (LD) 2fly; and 6 nmol/kg/min, high dose (HD) 2fly.

The nitric oxide-mediated smooth muscle relaxation by endothelium-dependent (2fly, acetylcholine, calcium ionophore (A23187)) and –independent (nitroprusside) agonists in aortas from these mice were recorded while contracted by a thromboxane A₂ agonist under isometric tension conditions in myographs. **Objective 1** was to characterize the dose and time effects of *in vivo* PAR₂-AP treatment on the subsequent vascular reactivity of aortas as a measurement of endothelial and smooth muscle cell health. **Objective 2** was to characterize the nitric oxide component of relaxations by measuring the agonist relaxation activity in chronic PAR₂-AP treated mice using pharmacological inhibitors of endothelial nitric oxide synthase (N ω -nitro-L-arginine-methyl ester, L-NAME) and cyclooxygenases (indomethacin). Based on initial experiments, it was apparent that chronic PAR₂-AP treatments attenuated the aortas relaxations induced by 2fly, ACh and nitroprusside in C57. **Objective 3** was to identify the possible mechanisms underlying the attenuated relaxations by PAR₂-AP. Western blotting of aortic proteins and immunohistochemical staining of aortas for PAR₂ were used to measure the expression levels of endothelial NO synthase (eNOS), soluble guanylyl cyclase (sGC), cyclooxygenases isoforms -1 and -2 (COX-1, COX-2), and PAR₂ to investigate the contributions of these components in attenuated relaxations.

To test **Hypothesis 2**, we used the chronic PAR₂-AP treatment model described above. **Objective 4** was to test whether high dose PAR₂-AP administered chronically lowered blood pressures in mice. To do this we recorded continuously the blood pressures and locomotor activity by radiotelemetry while administering the high dose PAR₂-AP to

mice.

From these studies, we expected to determine the effects of chronic treatment with PAR₂-AP on the endothelium function of mouse aortas and on the blood pressures, heart rates, and locomotor activities of mice.

Chapter 2: Literature Review

2.1 Proteinase-activated receptors (PARs)

Proteinase-activated receptors are a class of seven transmembrane domain G-protein coupled receptors, which consists of a family of 4, numbered 1 to 4 according to order of discovery (reviewed in Hollenberg, 2003). In the cardiovascular system, PAR are found on platelets (PAR₁, PAR₃ and PAR₄; Kahn *et al.*, 1998; Vu *et al.*, 1991), endothelial cells (PAR₁, PAR₂, and PAR₃; D'Andrea *et al.*, 1998; Hamilton *et al.*, 2002), smooth muscle cells (PAR₁ and PAR₂; D'Andrea *et al.*, 1998; Hamilton *et al.*, 2002), cultured cardiomyocytes (PAR₁, PAR₂, and PAR₄; Hamilton *et al.*, 2002, Ide *et al.*, 2007, and Sabri *et al.*, 2003), megakaryocytes (PAR₃ and PAR₄; Ishihara *et al.*, 1997 and Kahn *et al.*, 1998), leukocytes (PAR₂; Dery *et al.*, 1998) and fibroblasts (PAR₁; Connolly *et al.*, 1996).

The normal structure of PAR conceals a tethered ligand that is exposed by serine proteinases cleaving the N-terminal domain of PAR. Table 2.1 contains the N-terminal amino acid sequences of the revealed tethered ligands in mice, rats, and humans. The N-terminus binds to a region of extracellular loop 2, which induces a conformational change in the receptor that couples with activation of several possible G-proteins (reviewed in

Receptor	Revealed tethered ligand sequence
PAR ₁	(human) SFLLRN... (rat, mouse) SFFLRN...
PAR ₂	(human) SLIGKV... (rat, mouse) SLIGRL...
PAR ₃	(human) TFRGAP... (mouse) SFNGGP...
PAR ₄	(human) GYPGQV... (mouse) GYPGKF... (rat) GFPGKP...

Table 2.1 Tethered ligand sequences from human, rat, and mouse for each member of the PAR family. Modified from Hansen *et al.*, 2008.

Macfarlane *et al.*, 2001). Selectivity for the activation of PARs amongst serine proteases (a superfamily of enzymes) has been identified: for example, thrombin activates PAR₁, PAR₃, and PAR₄, but not PAR₂ (MacFarlane *et al.*, 2001). PAR-activating peptides (PAR-AP) mimic the tethered ligand sequence and so are substituted as more practical pharmacological tools than enzymes (Dery *et al.*, 1998; Hollenberg *et al.*, 1997; Hollenberg *et al.*, 1999). Figure 2.1 illustrates these two mechanisms for PAR₂ activation: 1. Cleaving the N-terminus produces PAR₂-tethered ligand, and 2. binding of extracellular loop 2 by PAR₂-AP.

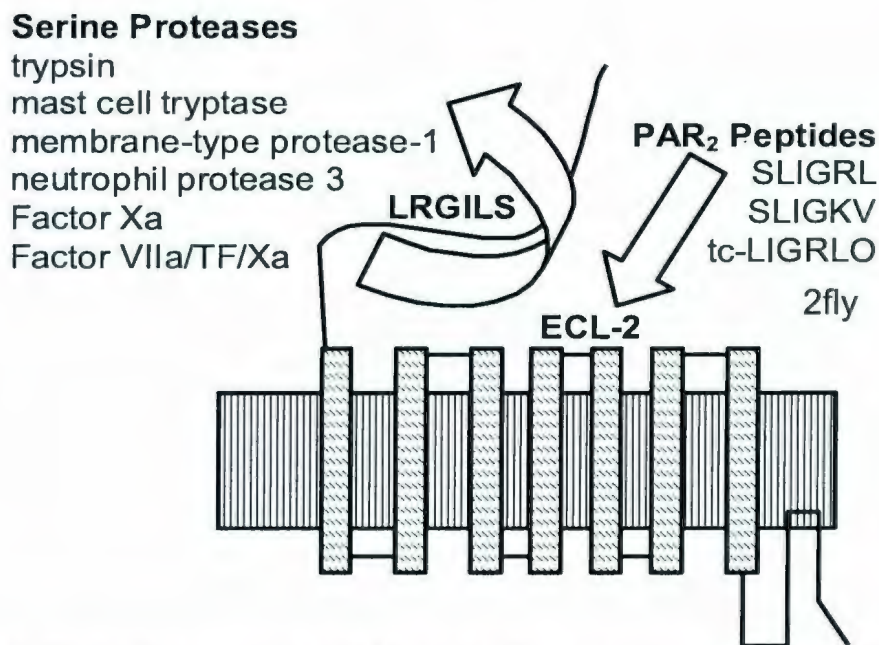


Figure 2.1 Illustration comparing PAR₂ activation by enzymes versus PAR₂-AP.

Modified from McGuire (2004). Used with author's permission.

2.2 PAR₂-activating peptides

Several of the more common PAR-APs are listed in Table 2.2. 2-furoyl-LIGRLO-NH₂ (2fly) has proven to be one of the most potent and specific agonists that have been purposefully designed to target PAR₂. 2fly is 10 to 300-times more potent than SLIGRL-NH₂, the native amino acid sequence of the exposed region in rats and mice (Table 2.2) (McGuire *et al.*, 2004a). The substitution of serine by a furoyl group and the addition of ornithine to the carboxy terminus of SLIGRL contribute to increased potency and a resistance to aminopeptidases. In total, 2fly is a more effective PAR₂-AP compared to

what we refer to as legacy PAR₂-AP.

PAR ₁	PAR ₂	PAR ₃	PAR ₄
SFLLRN-NH ₂	SFLLRN-NH ₂	TFRGAP ^a	GYPGQV-NH ₂
TFLLR-NH ₂	SLIGKV-NH ₂		GYPGKF-NH ₂
TFRIFD	SLIGRL-NH ₂		AYPGKF-NH ₂
	transcinnamoyl-LIGRLO-NH ₂		
	2-furoyl-LIGRLO-NH ₂		

Table 2.2 PAR-activating peptides. Peptide sequences are abbreviated by the internationally accepted biochemical nomenclature standard using the 1 letter code for each amino acid. Exceptions, NH₂ = amide functional group. Though not listed separately, it is common to find that studies have used the free carboxylic acid forms, which have 10-times less potency than the amides. ^a Although this is the reference for the tethered ligand sequence, it has not been found to activate PAR₃.

2.3 Cardiovascular actions of PAR₂-APs

A potentially promising therapeutic activity of PAR₂-APs is that these compounds can produce endothelium-dependent relaxation of vascular smooth muscle cells (Al-Ani *et al.*, 1995). In acute *in vivo* studies PAR₂-AP caused a reduction in blood pressure without increasing heart rate in anaesthetized rats (Emilsson *et al.*, 1997) and mice (Cheung *et al.*, 1998) using SLIGRLETQPPI and SLIGRL-NH₂ respectively. It was reported by McLean *et al.* (2002) that PAR₂ activation was protective against myocardial

ischemia and reperfusion injury. This protection occurred because PAR₂-AP infusion increased coronary perfusion despite being unresponsive to acetylcholine under these conditions (McLean *et al.*, 2002). Robin *et al.* (2003) administered i.v. SLIGKV-NH₂ to healthy volunteers while measuring blood flow in the forearm. They reported no adverse effects and that SLIGKV-NH₂ increased blood flows. These increases by SLIGKV-NH₂ were reduced (26%) by pretreatment by N^G-methyl-L-arginine and were reduced even more by combining the later with aspirin.

In various animal models of human diseases, PAR₂ mediated vasodilation is preserved despite other endothelium-dependent vasodilators being less effective. In genetic hypertensive mice (BPH/2) relaxation of small mesenteric arteries by PAR₂-AP were only slightly reduced (6%) when compared to normotensive mice (BPN/3) (McGuire *et al.*, 2007). In contrast, relaxations by acetylcholine and bradykinin in BPH/2 were significantly reduced by 25-50% compared to BPN/3 (McGuire *et al.*, 2007). This preservation of PAR₂ function in the small calibre arteries was attributed to an endothelium-dependent hyperpolarization mechanism. In basilar (Sobey *et al.*, 1999) and pulmonary arteries (Wanstall and Gambino, 2004), the preserved PAR₂ relaxations were nitric oxide (NO) mediated in SHR and pulmonary hypertensive rats, respectively. Similar to the findings by McGuire *et al.* (2007), stroke prone hypertensive rats (SHR) displayed reduced middle cerebral artery vasodilation by bradykinin and A23187 while 2fly-induced vasodilation remained unchanged (Smeda and McGuire, 2007). According to PAR₂ immunostaining of middle cerebral arteries there was no apparent change in

distribution of PAR₂ expression (Smeda *et al.*, 2010). When taken together, these studies reveal that PAR₂-AP could play a number of cardioprotective roles. The acute lowering of arterial blood pressures is one protective role. The maintenance of the capacity for endothelium-dependent relaxation despite reduction in effectiveness of other vasodilators in disease models is a second protective role.

2.4 *In vivo* effects of PAR₂-AP link with inflammation and immunity

PAR₂ activation *in vivo* can cause both anti-inflammatory and pro-inflammatory effects as well as change expression of molecules associated with immune mechanisms. Anti-inflammatory effects have been measured by acutely administering *in vitro* and *in vivo* PAR₂-APs. One early *in vitro* study of PAR₂-APs infused SLIGRL-NH₂ in a rat model of myocardial ischemia reperfusion injury (isolated perfused working hearts). This caused an increase in myocardial contractile recovery and decreased oxidative stress from free radicals during reperfusion in the ischemic risk zone (Napoli *et al.*, 2000). In the respiratory system, intranasal administered SLIGRL inhibited antigen-induced hyper-reactivity and infiltration of eosinophils in the airway (De Campo and Henry, 2005). SLIGRL administered *in vivo* also increased prostaglandin E₂ levels in the bronchiolar lavage (a mechanism in the lung that reduces inflammation by reducing inflammatory molecule recruitment (Lan *et al.*, 2001; Vancheri *et al.*, 2004)) in the absence of any inhibitors. When PAR₂-AP was co-administered with indomethacin (blocking prostaglandin E₂ production) the allergy hyper-responsiveness returned (De Campo and Henry, 2005). Intrarectal administered SLIGRL-NH₂ was found to protect against

experimental colitis that had been induced by exposure to trinitrobenzene sulfonic acid (Fiorucci *et al.*, 2001). This protection by PAR₂-AP was described by increased macroscopic and histological scores and reduced level of T helper 1 type cell cytokines (Fiorucci *et al.*, 2001). These studies demonstrate the ability of PAR₂ to elicit anti-inflammatory effects. The latter two studies also display differences in the modulation of immune mechanisms. The activation of PAR₂ caused changes in the amount of mediators of the immune response, an increase in prostaglandin E₂ (an anti-inflammatory effect in the lungs) and a decrease in T helper 1 type cell cytokines.

In vivo administered PAR₂-AP can cause pro-inflammatory effects. Injection of SLIGRL-NH₂ into rat paws caused oedema resulting from increased vascular permeability (Kawabata *et al.*, 1998; Vergnolle *et al.*, 1999). The oedema in these rats was characterized as being independent of mast cell activation and of the production of prostanoids and NO. These features of inflammation were demonstrated in hind paw oedema using compound 48/80 (depletes mast cells), cromolyn (a mast cell stabilizer), indomethacin, and L-NAME, respectively (Vergnolle *et al.*, 1999). Increased inflammatory response described by joint swelling and synovial vasodilation has also been reported to occur in mouse knee joints that had been administered either SLIGRL-NH₂ or 2-furoyl-LIGKV-OH (Ferrell *et al.*, 2003). Local intracolonic administration of SLIGRL-NH₂ caused inflammation as described by increased wall thickness and macroscopic damage score, caused increased tumor necrosis factor- α , IL-1 β , and interferon- γ mRNA expression (increase in T-helper 1 cells) and caused increased

epithelial permeability (Cenac *et al.*, 2002). PAR₂-AP 2fly administered to rats prior to intestinal irradiation exacerbated the tissue injury at early time points following exposure (Wang *et al.*, 2010). These studies show that PAR₂ activation *in vivo* has potential to increase pro-inflammatory effects at multiple sites and has been associated with immunity regulated by T-helper 1 cells.

2.5 PAR₂ antagonists

To understand the consequences of PAR₂ activation more clearly, PAR₂ antagonists would be of great use. Researchers have synthesized antagonists of PAR₁ that have been characterized by their ability to inhibit both the initial transient global cytosolic calcium signal and endothelium-mediated relaxation (reviewed in Ahn *et al.* 2003). However, there has been limited success in developing an antagonist to PAR₂. One approach used to develop PAR₂-antagonist compounds was functional screening of peptides comprised of the reversed amino acid sequence of the PAR activating peptides. Al-ani *et al.* (2002) attempted this approach for both PAR₁ and PAR₂ using FSLLRY-NH₂ and LSIQRL-NH₂ respectively. These peptides were previously described as having no PAR agonist activity (Al-ani *et al.*, 1999). FSLLRY-NH₂ and LSIQRL-NH₂ blocked trypsin activation of PAR₂, but did not block SLIQRL-NH₂ mediated activation of calcium signaling in Kirsten virus-transformed kidney cells or relaxation of rat aorta (Al-ani *et al.*, 2002). Other approaches to develop inhibitors of PAR activities include peptidomimetic molecules (Ahn *et al.*, 2003), pepducins (Kaneider *et al.*, 2007), small interfering ribonucleic acid sequences (siRNA), and monoclonal antibodies (Kelso *et al.*,

2006).

Mimetic molecules for PAR₁ inhibition are compounds that resemble the chemistry of the same binding motif as the activating amino acid sequences, the template being a 6-aminoindole ring. One such antagonist is RWJ-58259, which binds with high affinity and inhibits PAR₁ mediated platelet aggregation (Ahn *et al.*, 2003). The inhibitor actions of PAR₁ small-nonpeptide inhibitors including pyrroloquinazoline analogs, benzimidazole derivatives, and himbacine analogs have also been described (Ahn *et al.*, 2003). Generally, pepducins can have either agonist or antagonist activity by interacting intracellularly with the G-protein coupled pathways. These compounds have been successfully employed as agonists to both PAR₁ (Kaneider *et al.*, 2007) and PAR₂ (Covic *et al.*, 2002; Kaufmann *et al.*, 2009), but not as PAR antagonists. siRNAs, antibodies (B5 antibody specifically), and *N*1-3-methylbutyryl-*N*4-6-aminohexanoyl-piperazine (ENMD-1068) have been successfully employed to partially inhibit PAR₂ activation (Kelso *et al.*, 2006). siRNAs reduced the amount of knee joint swelling after cytokine induction. The B5 antibody serum also reduced knee joint swelling in mice after induction of inflammation via carrageenan/kaolin (Kelso *et al.*, 2006). ENMD-1068 reduced calcium signaling in Lewis lung carcinoma cells mediated by SLIGKV-NH₂, but had no effect on trypsin activation in these cells (Kelso *et al.*, 2006), and thus, was a partial antagonist.

In the past two years there has finally been some progress made in discovery of small molecule inhibitors of PAR₂. One study, by Kanke *et al.* (2009) described two new peptidomimetic antagonists of PAR₂ (K-12940 and K-14585). Both antagonists reduced

SLIGKV-induced calcium influx in primary human keratinocytes and inhibited competitively the specific binding of [³H]-2-furoyl-LIGRL-NH₂ to the cell membrane (Kanke *et al.*, 2009). Competitive inhibition of SLIGRL-induced relaxation of rat aorta was reported with K-14585 (Kanke *et al.*, 2009). The most recent study, by Barry *et al.* (2010), described the first compound (GB83) to inhibit PAR₂ activation via proteinases and by synthetic peptides (2fly) at low concentrations. GB83 was shown to inhibit PAR₂ induced intracellular calcium release in a colon cancer cell line in a dose dependent manner with full potency at μM concentrations.

It has taken many years to develop an antagonist of PAR₂ that has the ability to inhibit activation by proteinases and synthetic peptides. It is expected that GB83 should prove to be very useful to further describe the actions of PAR₂ and the consequences of blocking the receptor.

2.6 PAR₂ knockout mice

Prior to discovery of pharmacological inhibitors of PAR₂, transgenic PAR₂^{-/-} mice have been used to investigate the *in vivo* role of PAR₂ in various experimental models of diseases. Several strains of PAR₂^{-/-} mice have been used to investigate the cardiovascular actions of PAR₂ (Damiano *et al.*, 1999; McGuire *et al.*, 2002a; McGuire *et al.*, 2008) and inflammatory models of disease (Cenac *et al.*, 2002; Ferrell *et al.*, 2003; Kelso *et al.*, 2006; Lindner *et al.*, 2000; Schmidlin *et al.*, 2002; Seeliger *et al.*, 2003).

Cardiovascular phenotype characteristics present in PAR₂^{-/-} include higher systolic arterial pressures and pulse pressures compared with C57 (PAR₂^{+/+}) under baseline

conditions when measured by radiotelemetry (McGuire *et al.*, 2008). These mice have also been used to demonstrate that hypotension produced by acute i.v. administered SLIGRL-NH₂ in wild type mice was due to PAR₂ expression (Damiano *et al.*, 1999).

There are differences in PAR₂^{-/-} responses in various models of inflammation which creates some uncertainty about the pathophysiological role that may be played by PAR₂. PAR₂^{-/-} mice are protected from airway inflammation (Schmidlin *et al.*, 2002), contact dermatitis (Seeliger *et al.*, 2003), and colitis (Lindner *et al.*, 2000). The inflammatory response is substantially less in mouse knee joints of PAR₂^{-/-} compared to their wild type counterpart after adjuvant induced arthritis (Ferrell *et al.*, 2003). In this arthritis model PAR₂^{-/-} mice had lowered swelling compared to wild type. Intracolonic administration of SLIGRL-NH₂ caused little change in inflammation of PAR₂^{-/-} mice as compared to PAR₂^{+/+} mice (Cenac *et al.*, 2002). PAR₂^{+/+} had increased wall thickness and macroscopic damage score, increased tumor necrosis factor- α , IL-1 β , and interferon- γ mRNA expression (increase in T-helper 1 cells) and increased permeability (Cenac *et al.*, 2002). In general, PAR₂^{-/-} responses to immune system action are lower than PAR₂^{+/+}, but there is contradictory evidence that indicates that injury and inflammatory responses in some cases were increased in PAR₂^{-/-}.

Increased inflammation was observed after acute focal ischemic brain injury as PAR₂^{-/-} mice compared to their counterparts had an increased infarct volume (Jin *et al.*, 2005). In pancreatitis there seems to be different effects that are dependent on the mechanism of inducing inflammation. Induction of pancreatitis by a supramaximal

caerulein stimulation caused increased inflammation in PAR₂^{-/-} mice (Sharma *et al.*, 2005) whereas the inflammation induced by retrograde administration of bile salts in the pancreatic duct was reduced in PAR₂^{-/-} (Laukkarinen *et al.*, 2008). These findings are evidence that PAR₂^{-/-} mice may exhibit different outcomes, sometimes opposite, depending on the tissues and experimental model studied. For our purposes it is important to know that PAR₂^{-/-} can exhibit different inflammatory responses when stimulated.

2.7 Endothelium-dependent relaxation mechanisms

An understanding of vasodilator mechanisms similar to those produced by PAR₂ activation, such as endothelium-dependent relaxation by cholinergic agonist acetylcholine and calcium ionophore A23187, is useful to designing studies to characterize potential signal transduction mechanisms underlying PAR₂ responses.

In what are now considered classic *in vitro* experiments, the neurotransmitter acetylcholine was found to relax precontracted rabbit aortas (Furchgott and Zawadzki, 1980). Relaxation was dependent on the presence of intact endothelial cells because when inner surfaces of rabbit aortas were damaged by rubbing, relaxation did not occur (Furchgott and Zawadzki, 1980). These fundamental observations led to the co-award of the 1998 Nobel Prize in Medicine to Furchgott, Ignarro, and Murad; the work of the latter two contributed to the identification of (NO) being the mediator of this endothelium-dependent relaxation and the role of soluble guanylyl cyclase in signal transduction, respectively (SoRelle, 1998).

Acetylcholine activates the type 3 muscarinic receptor (M3) found on endothelial

cell plasma membranes (Dauphin and Hamel, 1990). M3 cholinoreceptor is a classic seven transmembrane domain G-protein coupled receptor. Briefly, activation of M3 receptors causes $G\alpha_q$ to exchange GDP for GTP. $G\alpha_q$ is released from its $G\beta\gamma$ subunit which acts as the signal transduction molecule leading to activation of phospholipase C. Phospholipase C cleaves phosphatidylinositol-4, 5-bisphosphate into inositol triphosphate and diacylglycerol (Noh *et al.*, 1995). Inositol triphosphate binds to its nominal receptor on the endoplasmic reticulum that causes a release of stored Ca^{2+} into the cytosol of endothelial cells (Noh *et al.*, 1995). Ca^{2+} binds to calmodulin to activate endothelial nitric oxide synthase (eNOS) (Matsubara *et al.*, 1996). NO synthases catalyse the oxidation of L-arginine to L-citrulline while producing diffusible free radical gas NO (Kwon *et al.*, 1990). NO diffuses into the smooth muscle cells where it binds to and activates soluble guanylyl cyclase, which converts GTP to cGMP. The accumulation of cGMP leads to activation of cyclic GMP-dependent protein kinases and subsequent phosphorylation of various substrates linked to the regulation of Ca^{2+} including those mediating sequestration by the sarcoplasmic reticulum (Twort and Breemen, 1988), Ca^{2+} desensitization (Stull *et al.*, 1990; Tansey *et al.*, 1992), and plasma membrane Ca^{2+} extrusion from the smooth muscle cell (Popescu *et al.*, 1985).

A23187 is a calcium ionophore that has blood vessel relaxant activity, that is dependent (in a concentration dependent manner) on the presence of an endothelium layer (Furchgott, 1983). It has a different mechanism of action than acetylcholine. A23187 forms pores in the membrane of endothelial cells that allow the entry of Ca^{+2} into the

cells (Reed and Lardy, 1972). It is proposed that this stimulates the production of NO, which follows the same pathway as NO derived by eNOS, to cause relaxation through sGC.

PAR₂-AP mediated endothelium-dependent relaxation of large calibre arteries occurs by a mechanism which resembles that underlying the typical acetylcholine- and A23187-induced relaxations. In large arteries NO is the mediator of the PAR₂ signal transduction mechanism (Figure 2.2). In small resistance calibre arteries, endothelium agonists including PAR₂-AP (McGuire *et al.*, 2002; McGuire *et al.*, 2004a), acetylcholine and A23187 do not necessarily require NO to cause vasodilation. In the presence of NOS inhibitors, for example L-NAME, SLIGRL-NH₂ and other PAR₂-APs induce the relaxation of small mesenteric arteries contracted by a vasoconstricting agonist (McGuire, 2002). These responses are mediated by endothelium-dependent hyperpolarization (EDH) of vascular smooth muscle, which involves activation of small- and intermediate-conductance Ca²⁺-activated K⁺ channels on the endothelium (McGuire *et al.*, 2002a; McGuire *et al.*, 2002b; McGuire *et al.*, 2004a; McGuire *et al.*, 2004a). This alternate EDH cascade may provide a mechanism for vasodilation of arteries in disease states when NO is limited.

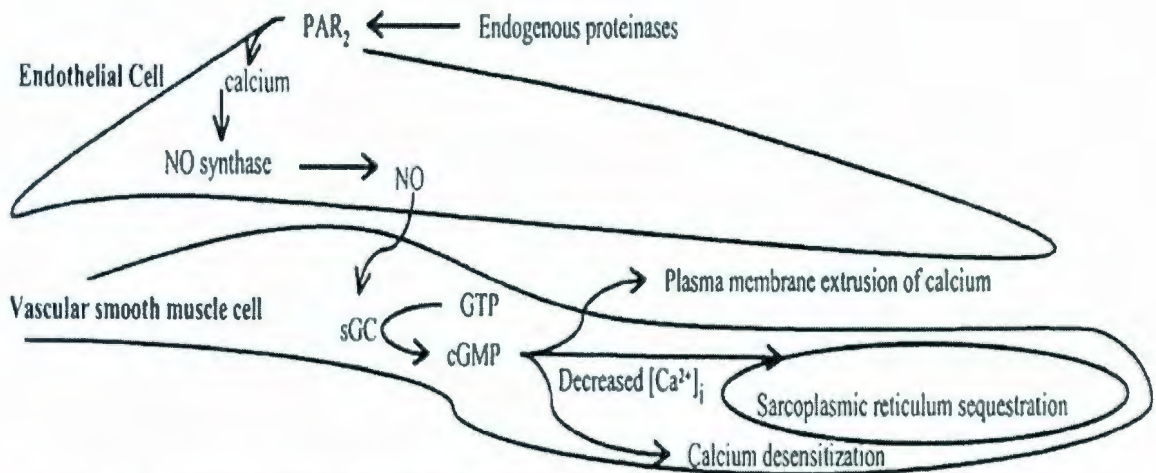


Figure 2.2 Vascular smooth muscle relaxation by PAR₂ activation via endothelial-derived NO. Used with the author's permission (McGuire, 2004).

2.8 Endothelium-independent nitrovasodilators

Nitroprusside initiates its vasodilator action upon spontaneous release of NO (Rao and Cederbaum, 1995). Thus, nitroprusside provides an exogenous source of diffusible NO that causes smooth muscle to relax. The mechanism of action of nitroprusside bypasses the endothelium and the activation of eNOS, but still involves activation of soluble guanylyl cyclase and cyclic GMP-dependent protein kinase activation. Nitroprusside is frequently used as a tool for comparing relaxation by endothelium-dependent and -independent mechanisms.

2.9 Non-hemodynamic effects of PAR₂-AP on endothelial cells

There has been much work performed on endothelial cells to try to describe how PAR₂ mediates its actions within *in vivo* and *in vitro* systems. These studies have found PAR₂-APs also have many non-hemodynamic effects on endothelial cells, including

stimulating the production of pro-inflammatory molecules and other mediators of the innate immune system. Activation of PAR₂ also increased the release of prostanoids and cytokines (IL-6 and IL-8) in epithelial and non-epithelial cells (Lourbakos *et al.*, 2001). PAR₂ activation in cell lines is partly linked to the NFκB pathway (Buddenkotte *et al.*, 2005; Goon Goh *et al.*, 2008; Kanke *et al.*, 2001; Macfarlane *et al.*, 2005) involved in the regulation of IL-8 production (Yoshida *et al.*, 2007). Also the activation of p38 MAP kinase and NFκB by PAR₂-AP in human umbilical vein endothelial cells has been reported (Ritchie *et al.*, 2007). PAR₂ expression can be upregulated by tumor necrosis factor-α, IL-1β, and lipopolysaccharide in human umbilical vein endothelial cells (Nystedt *et al.*, 1996). Together these observations imply evidence linking PAR₂ to pro-inflammatory actions of endothelial cells.

2.10 Methods for assessment of endothelial dysfunction

In a clinical setting there are several technical methods to assess endothelial dysfunction. The typical approach has involved recording hemodynamic responses by acetylcholine, bradykinin and or endothelium-independent nitrovasodilators. It is proposed that an attenuated responsiveness to all of these drugs is enough to demonstrate endothelial dysfunction. For example, quantitative coronary angiography (Cox *et al.*, 1989) is employed to visualize blood vessels vasodilations by these agonists (Schachinger *et al.*, 2000). Alternate methods have been proposed, which include recording the coronary arteries responses to cold pressor testing (Schindler *et al.*, 2003) and flow-mediated vasodilation of large arteries of the forearm vascular bed (Perticone *et al.*, 2001)

or microvasculature (skin microcirculation) using laser Doppler techniques (Deanfield *et al.*, 2005). Another minimally invasive test is to observe the blood pressure (BP) changes occurring during reactive hyperemia using ultrasound and a BP cuff (Celermajer *et al.*, 1992). The premise behind following reactive hyperemia is that in patients with normal vascular function blood flow increases after occlusion, but in patients with endothelial dysfunction the vessel of interest does not relax to the same extent to permit an increase in blood flow (hyperemia). In line with the increasing clinical trend to measure molecular markers of disease (biomarkers) there are multiple markers that have been proposed to assess endothelial dysfunction in humans, which include IL-6, tumor necrosis factor- α , and C reactive protein (Deanfield *et al.*, 2005).

In vitro experiments have been performed on arteries isolated from gluteal tissue of human patients. There was reported in these studies a good correlation to the degree of flow-mediated dilation of the patient's brachial artery (Endemann and Schiffrin, 2004). Most *in vitro* research exploring mechanisms of endothelial dysfunction has been performed using animal models for ease of access and range of disease models available. For example, isolated vessels from rodents have been tested for effectiveness of acetylcholine to cause vasodilation under different conditions or stages of disease. Specific models include: spontaneously hypertensive rats (Luscher, 1988; Luscher, 1989), third order mesenterics from the two-kidney one-clip hypertension model in rats (Dohi *et al.*, 1991), angiotensin II hypertension model in rats (Rajagopalan *et al.*, 1996), and diabetic models in rats and rabbits (Cameron and Cotter, 1992; Tesfamariam *et al.*, 1989).

The effectiveness of acetylcholine is also reduced in mice models including hyperhomocystinemia (Viridis *et al.*, 2003). Endothelial dysfunction associated with cytokine production (tumor necrosis factor- α and IL-1B) derived from chronic PAR₂ activation has yet to be determined.

Chapter 3: Materials and Methods

3.1 Animal Ethics

The procedures on mice were approved by the Institutional Animal Care Committee of Memorial University in accordance with the guidelines and principles of the Canadian Council on Animal Care.

3.2 Materials

2fly (PAR₂-AP) and TFLLR-NH₂ (PAR₁-AP) were purchased from Peptides International (Louisville, KY). Antibodies SC-2020 (COX-2 secondary antibody), SC-1745 (COX-2 primary antibody), SC-25778 (GAPDH-FL primary antibody), and SC-13504 (PAR₂ primary antibody, (SAM-11)) were purchased from Santa Cruz Biotechnology. Antibodies labeled 160109 (COX-1 primary antibody), and 10004301 (COX-1 and GAPDH-FL secondary antibody) were purchased from Cedarlane (Burlington, ON). Antibodies for eNOS were purchased from BD Transduction Laboratories (primary antibody, 610296) and Vector Laboratories (secondary antibody, PI-2000). Antibodies for sGC were purchased from Abcam (primary antibody, ab5033) and Vector Laboratories (secondary antibody, PI-1000). Oligonucleotide primers for genotyping were purchased from Eurofins MWG Operon (Huntsville, AL). Sybr® Safe

was purchased from Invitrogen (Burlington, ON). For PCR experiments, Taq polymerase, MgCl₂, DNase-free water and 10 x PCR buffer were purchased from Bio Basic Inc. (Ontario, Canada). Fluorescein isothiocyanate (FITC)-conjugated AffiniPure goat anti-mouse IgG (115-095-003) was purchased from Jackson ImmunoResearch Laboratories (West Grove, PA, USA). All other chemicals were purchased from Sigma Aldrich Canada (Oakville, ON).

3.3 Mice

C57BL/6J (C57) and homozygous B6.Cg-*F2r11*^{tm1Mslb}/J (PAR₂^{-/-}) were obtained from The Jackson Laboratory (Bar Harbor, ME). Three PAR₂^{-/-} breeding pairs were used to generate an initial colony. C57 mice were purchased at intervals to age-match the PAR₂^{-/-} used in experiments. Male mice (12 to 20 weeks of age) were used in all experiments. Mice were housed within a specific-pathogen free barrier facility until used for experiments, and thereafter, mice were housed in a room dedicated for the main use of radiotelemetry recording. Room temperatures, humidity and light cycles were controlled by Animal Care Services in the Health Sciences Centre, but were monitored routinely for seasonal or unexpected (power blackouts) variations.

3.4 Breeding Protocol

The colony of PAR₂^{-/-} mice was started with three founding pairs from different parents. These breeding pairs produced about one litter of offspring every three to four weeks. Litter size varied from one to seven offspring. Litters were weaned on day 21 after birth. The litters from the pairs of breeders were then bred together to establish a stable

colony. The colony number was maintained while ensuring there was no breeding between relatives at least as far back as two generations. Eighteen months after the start of breeding the first pairs of PAR₂^{-/-}, the rate of colony growth appeared to slow. A decision was made to reestablish the PAR₂^{-/-} by backcrossing to C57 followed by breeding heterozygotes. Four pairs of female PAR₂^{-/-} of different family lines were mated to male C57 to generate first familial (F1) generations of heterozygote mice (PAR₂^{+/-}). These PAR₂^{+/-} from each pair were then crossbred (using both males and females from each breeding pair in combination) to create second familial (F2) generations of PAR₂^{-/-}, PAR₂^{+/-}, and C57 littermates. All mice from heterozygote crosses were genotyped to determine identity using tail clips.

3.5 Genotyping

Mice were genotyped using a modification of the supplier's recommended protocol (Jackson Laboratory, Bar Harbor, ME). Dideoxyribonucleic acid (DNA) extraction procedure entailed heating a mouse tail clipping (5 mm length) in a 500 µl solution of 50 mM NaOH for 1 h, cooling to room temperature, adding 50 µl TrisHCl (pH 7.5) followed by mixing and centrifugation at 10,000 x g for 2 min. The supernatant containing DNA was stored at -20 °C. DNA concentration was determined using the NanoDrop 1000 spectrophotometer (Fisher Scientific), which was calculated by the measured absorbance at 260 nm ($A_{260\text{nm}}$) by nucleic acids.

Polymerase chain reactions using 2 primer sets and a reaction mixture was used to amplify DNA. When paired correctly and at the optimal cycling conditions these primers

amplified the portions of DNA that were of interest (Appendix A). The reaction mixture amplified both a portion of the *par2* exon and the neomycin gene present in the PAR₂^{-/-} mice. This approach differed from the supplier as our protocol used IMR 5332 as one of the primers while Jackson Laboratories used IMR 7415 to amplify this region. The neomycin gene insert was introduced during the derivation of the PAR₂^{-/-} mouse genotype at The Jackson Laboratories, and thus, it would be absent in C57. To control for contaminants in the PCR mixtures, a no DNA template control was analysed concurrently with regular DNA-containing samples. To ensure that the correct genotypes were visualised on gels a positive and negative control were included in all assays. The positive and negative controls contained DNA from known C57 and PAR₂^{-/-}, respectively.

Standard agarose gel electrophoresis and DNA dye staining protocols were used to separate and then visualize the amplified DNA samples in order to identify the polymerase chain reaction products based on base pair lengths. Gels cast were (14 cm x 12 cm x 0.5 cm) 1.5 % agarose (w/v) Tris borate ethylenediaminetetraacetic acid (TBE) buffer containing Sybr® Safe DNA chelating dye. A loading dye (to allow experimenter to watch the progress of the electrophoretic separation) was added to polymerase chain reaction products. A DNA ladder of 100 base pair increments was used as a reference to identify the size of PCR products in parallel lanes. Gels were run for ~1.5 h at 90 V which produced clear separation of the DNA ladder base pairs and movement of the DNA primers > 4 cm from their wells. Polymerase chain reaction product DNA were imaged using Alpha Imager® EP, which used trans-ultraviolet light to illuminate DNA bands that

were stained by Sybr® safe.

3.6 Radiotelemetry

Physiological parameters were recorded in unrestrained mice using a radiotelemetry approach. Telemeters (TA11PA-C10, Data Sciences Inc.) were implanted following procedures described for recording blood pressure in aorta with access through the left carotid artery (McGuire et al., 2007). Telemeters were implanted into male mice 12-16 weeks of age, which weighed 22-34 g. Surgical procedures were 40-60 min and were followed by close observation for 48 h immediately after initial recovery from anesthesia. Recovery surgery was performed using a 3-stepped combination of isoflurane and oxygen anesthesia: induction: 100% O₂ (0.5 – 1 L/min) + isoflurane (3 - 4 %), maintenance: 100% O₂ (0.8 – 2 L/min) + isoflurane (1 – 2 %), and recovery: 100% O₂ (1 – 2 L/min). The final positions of the gel-filled catheter tip of the TA11PA-C10 telemeters, which were inserted into the left carotid artery and secured in position with silk ligatures, were verified later at necropsy. The TA11PA-C10 telemeter body was slid into a lateral subcutaneous pocket that had been filled with 0.2-0.5 ml saline. Saline (0.2 ml s.c.) and Duplocillin LA (0.02 ml intramuscular) were administered after all surgical wounds were closed with sutures. After wakening from anesthesia, mice were returned to their own cages and then transferred to a small animal intensive care unit, which provided a controlled temperature (30 °C) and humidity environment with a stream of oxygen (1 L/min) for 48 h post-operation observation.

Mice were allowed a 10 day recovery period before their baseline radiotelemetry

data were recorded. Five days (days -4 to -1) of continuous telemetry data were recorded as baseline using the proprietary DSI acquisition system, sampling the 3 s average for each variable every 30 s to produce 2880 data points for each variable per 24 h period. It is the standard practice of our laboratory that mice with 24 h mean pulse pressures less than 20 mmHg were excluded from subsequent data analysis because below this blood pressure the values may not be reliable (Van Vliet *et al.*, 2006).

3.7 Blood pressure and activity data analyses

The variables measured by radiotelemetry in the unrestrained mice were mean (MAP), diastolic (DAP) and systolic arterial pressure (SAP), pulse pressure (PP), heart rate (HR) and locomotor activity. These data were exported into a Microsoft Excel worksheet-based template designed for routine analysis of telemetry data (HemoDynamic Statistics, 'HDstats' version 2006b-1.xls, July 2, 2006; Van Vliet *et al.*, 2006). This spreadsheet generates 500 statistics based on the recorded variables for each 24 h period. Data obtained on the day of pump implant (day 0) and cage change days (day 8 and 11) were excluded from analyses. Data points containing fewer than 3 mice were excluded from analyses. Baseline data were calculated from the total number of mice of each strain as shown in Table 8 (C57 n=6 and PAR₂^{-/-} n=8). The statistical test to compare baseline data between strains was a Student's t-test for unpaired data. Two way ANOVA (pump x time) was used to compare the 24 h mean variables and changes of variables from baseline data.

The change from baseline data = values recorded on day x (where x is the day of pump implant) – mean of the baseline data.

Microsoft Excel and GraphPad Prizm software were used to manage data, perform statistical comparisons and create graphs.

3.8 Subcutaneous drug delivery

Drug treatments were delivered by subcutaneous infusion using micro-osmotic pumps. Micro-osmotic pumps were filled with saline or peptide (2 μ l) then equilibrated 6-12 h at 37 °C as per manufacturer's instructions (Alzet). The micro-osmotic pumps were then implanted subcutaneously in anaesthetized mice through an incision on the dorsal neck into a small pocket filled with saline along the flank as described previously (McGuire *et al.*, 2008). Surgeries to implant micro-osmotic pumps lasted 5-10 min and were followed by 2 h of recuperation in the small animal intensive care unit for full apparent recovery. The anesthesia protocol was the same as for telemeter implants. Each mouse was also administered 0.2 ml of saline s.c. and 0.02 ml of Duplocillin LA (per ml, active portion contains 150,000 international units (IU) benzathine penicillin and 150,000 IU procaine penicillin, with methyl parahydroxybenzoate (1.2 mg) and propyl parahydroxybenzoate (0.13 mg) as preservatives) intramuscularly. After 2 h post-surgical recovery, the mice were returned to the room dedicated to radiotelemetry recordings in the animal care facility. Length of treatment (7, 14 days) and dose (low, LD and high, HD) of administered peptide were selected by choosing an appropriate micro-osmotic pump model and varying the concentration of drug in the pump reservoir (7 days: model

1007D, pump rate 0.5 $\mu\text{l/h}$; 14 day: model 1002, pump rate 0.25 $\mu\text{l/h}$). Concentrations of drug inside reservoirs were adjusted by dilution with bacteriostatic saline to match the dose delivery rate on the starting (pre-pump implant) weight basis for each mouse. Mice assigned to 2fly treatment received either HD (6 nmol/kg/min) or LD (2 nmol/kg/min). Since there were no literature references regarding chronic infusions with PAR₂-AP at the initiation of these studies in September 2008 and because of practical considerations (amount of drug required and solubility), doses of 2fly were chosen based on a range of molar doses that were estimated to be in the equipotent molar dose range of SLIGRL-NH₂ used in acute studies of blood pressure effects (a 1 min i.v. infusion of 0.1, 0.3, 1 μmol SLIGRL-NH₂ /kg in anaesthetized mice reduced MAP by 10-40 mmHg for up to 5 min (Cheung *et al.*, 1998)). We made an assumption that 2fly would be at least 100 - 300-times more potent than SLIGRL-NH₂ *in vivo* as it had been reported to be at least such *in vitro* (McGuire *et al.*, 2004a).

3.9 Isometric tension measurements of mouse aortas

Mice were euthanized by overdose inhalation with isoflurane followed by a blood withdrawal by cardiac puncture using a syringe containing heparin (100 U). Thoracic descending aortas (1-2 cm) were removed and stored in ice-cooled Krebs's solution until cleaned of fat and adherent tissues. Two to four sections per aorta (2 mm lengths) were cut and mounted on 200 μm diameter hooks in a 610 multi-myograph chamber (Danish Myograph Technologies, Aarhus, DK). Aortas were bathed in a physiological salt solution (pH 7.4) comprised of 114 mM NaCl, 4.7 mM KCl, 0.8 mM KH₂PO₄, 1.2 mM

MgCl₂·6H₂O, 2.5 mM CaCl₂·2 H₂O, 11 mM D-glucose, and 25 mM NaHCO₃, while bubbled continuously with 95 % O₂/ 5 % CO₂ at 37 °C. Tissues were equilibrated at resting tension for 30 min prior to addition of any drugs. A normalized resting tension was set similar to the methods adopted for small calibre arteries from mice (McGuire *et al.*, 2007), a procedure first developed by Mulvany and Halpern (1977) for rat small mesenteric arteries. A pilot study on mouse aortas indicated that in the hands of the author, an optimum acetylcholine-induced relaxation activity was achieved by a resting tension that was set to 90% of the internal circumference that was estimated to produce aorta wall stress equivalent to 7.98 kPa. Increasing concentrations of K⁺ were added to test the viability and responsiveness of the tissues. Contraction data were obtained using either single doses (90 mM) or a cumulative series of doses (30 mM, 60 mM, 90 mM, and 120 mM). High K⁺ concentration solutions were balanced for osmolality by removing equimolar amounts of Na⁺.

Tissue preparations that generated <4 mN/mm of force in response to exposure to any contractile agonist were excluded from analysis. Each myograph chamber contained 8 ml of solution so investigational compounds were diluted at least 1/100 (80 µl in 8 ml) by direct addition to the organ baths. Most compounds were dissolved in nanopure filtered distilled water except indomethacin and A23187, which were dissolved in 95 % ethanol/5% water and pure dimethyl sulfoxide, respectively.

Cumulative concentration-contraction response relationships were determined for phenylephrine (1 nM to 100 µM) and U46619 (1 nM to 1 µM). From these relationships

submaximal contractions (50-80%) were produced by addition of varying concentrations of U46619 (10 nM to 100 nM) rather than phenylephrine, which produced an average contraction <4 mN/mm of force. U46619-induced contractions were used to determine relaxation responses elicited by cumulative addition of various compounds. Such compounds included acetylcholine (1 nM to 100 μ M), nitroprusside (0.1 nM to 100 μ M), 2-furoyl-Leu-Ile-Gly-Arg-Leu-Orn-NH₂ (1 nM to 3 μ M), Thr-Phe-Leu-Leu-Arg-NH₂ (1 nM to 3 μ M), and A23187 (1 nM to 1 μ M). Inhibitors were incubated for 15 minutes prior to contraction. Inhibitors included L-NAME (300 μ M) and indomethacin (10 μ M).

Endothelium denudation of aortas was performed in order to investigate the endothelium-dependence of responses to specific drugs. Endothelial cells were damaged by rotating the aorta around the two hooks inside the myograph chambers. Resting (initial) tension was set by adjusting to the same length as prior to endothelium removal. Vessels were contracted by U46619 as before and acetylcholine, nitroprusside and 2fly (at concentrations above) were tested for endothelium dependence.

Continuous recording of isometric tension data were acquired via computer connections using MyoDaq/MyoData and ADI Instruments Chart 5 software packages. Data points representative of the maximal responses to each concentration of drug were selected and later exported to a master spreadsheet template file in Excel 2003.

3.10 Western Blots

Protein was collected by homogenization of aortas in lysis buffer B (0.8 x TBS, pH 7.4) containing 10 % (v/v) glycerol, 1 % (v/v) NP-40, 1 mM NaF, 1 mM Na₃VO₄,

0.025 % (w/v) SDS and a standard protease inhibitor cocktail) with a glass micro tissue grinder (Wheaton) on ice. Samples were centrifuged at 14,000 rpm for 15 min in a microcentrifuge (Centrifuge 5415C, Eppendorf) and the supernatants were collected for protein concentration determination. Protein concentrations of supernatants were determined using Pierce bicinchoninic acid assay kit (Fisher; # 23227) with automated FluroStar microplate reader according to the manufacturer.

Individual proteins were separated by relative molecular weight using routine SDS PAGE (10% SDS; 8 % polyacrylamide crosslinking). Supernatant protein was added to lysis buffer B plus loading buffer containing dithiothreitol (DTT). A protein molecular weight ladder (Benchmark Prestained protein ladder, Invitrogen) was run in a parallel lane to allow determination of the relative molecular weights of immunoreactive bands. A positive control lane containing protein isolated from mouse vas deferens was used to validate the relative molecular weight of immunoreactive bands corresponding to cyclooxygenase-1 (COX-1) and cyclooxygenase-2 (COX-2). Although the specific antibodies for sGC and eNOS were already well characterized by others in a variety of vascular tissues, we confirmed the specificities with homogenized lung samples from mice in separate experiments. All samples including the positive controls, but not the ladder, were boiled at 100 °C for 5 min prior to loading on gels. Gels were run at 120 V until the dye front reached the end of the gel.

Proteins were transferred from the gel to polyvinylidene fluoride membranes by electrophoresis (1.5 h at 100 V) in ice cold transfer buffer comprised of 25 mM Tris-base

(pH 8.3), 192 mM glycine, and 10 % methanol. Membranes containing the proteins were washed with TBST buffer; TBS (pH 7.4) containing 0.1% Tween-20) then blocked (15 min) with a solution of TBST containing 3% (w/v) bovine serum albumin. Membranes were probed with antibodies for the proteins of interest as given in Appendix B; optimal conditions (dilutions) for each antibody had been determined in previous work of the laboratory. The blocked membranes and primary antibodies were incubated together overnight at 4 °C and then washed 4-times with TBST. Then an appropriate secondary antibody-linked to horseradish peroxidase was incubated together with membranes for 1 h at room temperature (~25 °C) before exposure to substrate and visualization of immunoreactive bands by enhanced chemiluminescence on photographic film. The developed films were scanned (Hewlett-Packard ScanJet 3300C) using Adobe Photoshop v8 software and then a file copy was converted to a JPEG format. These files were imported into ImageJ software for densitometric analyses of bands.

3.11 Immunohistochemistry

Segments of saline and 2fly high dose-treated C57 and PAR₂^{-/-} aortas were stored in optimal cutting temperature gel and sectioned using a cryotome at -20 °C. Frozen 8 μm sections (rings) were placed on gelatin-coated slides. These slides were stored at -20 °C until final use. They were probed by a primary antibody, SAM-11, a monoclonal antibody raised against human N-terminus of PAR₂ (Molino *et al.*, 1997), at different dilutions (1/50, 1/100, and 1/500) of a stock solution (0.2 mg/ml). A secondary antibody (anti-mouse IgG) labeled with FITC (dilution of 1/500; stock solution 1.5 mg/ml) was used to

detect the primary staining distribution. The FITC fluorescence emission was measured in response to 492 nm excitation light from an argon laser. The emitted FITC fluorescence was filtered at 520 nm (peak of emission spectrum of FITC) and imaged by a confocal microscope (Olympus Fluoview, FV300). Stack images from a 10 μm depth of tissue sections were obtained by stepping up or down the confocal plan through the preparation (z step = 1 μm). Image analyses of 1 μm sections were performed by randomly selecting three areas of each stack image. Image J (line tool) was used to quantify the fluorescence patterns across the length of the vessel wall. This was measured as pixel density per length of aortic wall at each 1 micron step, in the section. The patterns of pixel density were compared between other sections of the same sample type to determine a common representation if such existed. These were then compared between treatment and strains.

3.12 Statistical Analyses

Graph Pad Prizm v4 was used to create all graphs and conduct the statistical analyses. Unless otherwise stated, the drug concentration response curves (CRC) for each aorta were fit by nonlinear regression to a four parameter logistic equation with a fixed origin set to 0. Three parameters: pD_2 , E_{max} , and Hill slope, were used to determine changes in sensitivity, maximal effectiveness, and changes in relaxation curve kinetics, respectively. Hill slopes were not restricted to allow for differences in drug interactions.

The equation is as follows:

$$\% \text{ relaxation} = \text{Bottom} + (E_{\text{max}} - \text{Bottom}) / (1 + 10^{(\log \text{EC50} - \log [2\text{fly} (M)]) * \text{Hill slope}}); \text{bottom, constant} = 0; E_{\text{max}}, \text{maximum \% relaxation}; \text{pD}_2, \text{negative}$$

logarithm base 10 of EC50 value.

Data that were not good fits ($R^2 < 0.8$) by the nonlinear regression method, e.g. some inhibitor treatments and A23187 responses, were analyzed using alternative or additional approaches as described in the appropriate section of results. Statistical comparison of the means of more than two independent groups were made by two way ANOVA (main effects were pump and time) and were followed by a Bonferroni post-hoc test. Statistical analysis of three groups with one independent variable was made by one way ANOVA. Statistical comparisons that involved the means of only two groups were made by Student's t-test for unpaired data. $P < 0.05$ was considered significant. (n) represents the number of independent samples i.e. n equals the number of mice per group. Error bars on graphs represent the standard error of mean.

Chapter 4: Results

4.1 Effect of chronic PAR₂ activation on NO-mediated relaxation of aortas

4.1.1 2fly Relaxation

We measured 2fly relaxation after chronic PAR₂-AP treatment and saline treatment to determine if these treatments affected PAR₂ reactivity in aortas. Chronic PAR₂-AP caused a 3- (LD) to 4-fold (HD) decrease in sensitivity for 2fly CRC in C57 aortas represented by decreased pD₂ values (Table 4.1) and a rightward shift in the curve (Figure 4.1A) at 7 days. At 14 days a 3-fold (LD) and a 2-fold (HD) difference was observed in pD₂ values as well as a rightward shift in the CRC (Figure 4.1B). The E_{max}

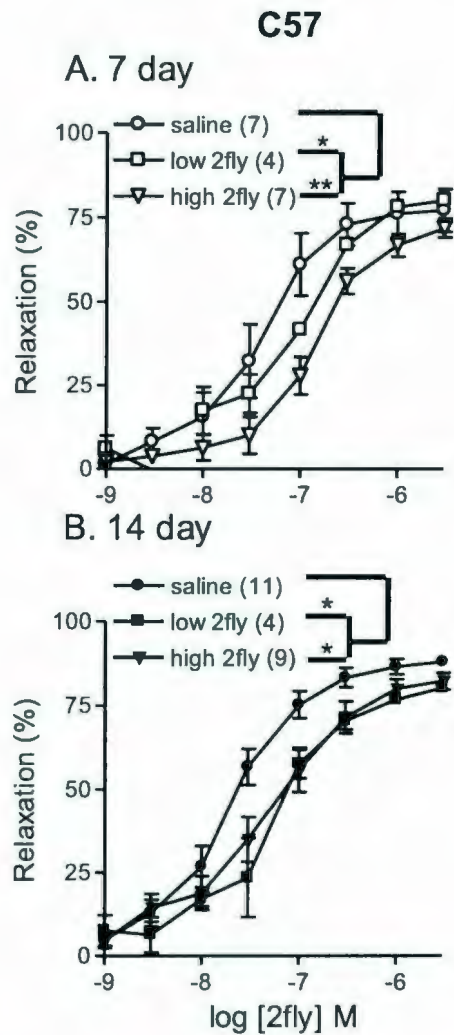


Figure 4.1. Effect of PAR₂-AP s.c. infusions for 7 (A) and 14 (B) days on 2fly-induced relaxations of isolated C57 aortas. Mice were implanted with 7 (A) and 14 (B) day pumps s.c. Isolated aortas were contracted submaximally (50-80%) by U46619 prior to determining relaxation by 2fly. Values in parentheses are the number of mice. * P<0.05 for pD₂, saline vs. low 2fly 7 days, saline vs. low and high 2fly 14 days and ** P<0.01 for pD₂, saline vs. high 2fly 7days 2way ANOVA, Bonferroni.

and hill slopes for 2fly CRC were not different between groups (Table 4.1). Aortas of $PAR_2^{-/-}$ mice showed no relaxation or contraction to cumulative addition of 2fly. These data indicate the decrease in PAR_2 -AP sensitivity in C57 was dependent on *in vivo* dose and length of infusions.

2fly		micro-Osmotic Pump Treatment											
Duration (days)	Artery Treatment	n	Saline			2fly low dose				2fly high dose			
			pD ₂ (M)	E _{max} (%)	Hill Slope	n	pD ₂ (M) ^{a,b}	E _{max} (%)	Hill Slope	n	pD ₂ (M) ^{a,b}	E _{max} (%)	Hill Slope
7	Control	7	7.5(0.1)	82(2)	3.1(1.6)	4	7.0(0.1) ^c	75(5)	0.8(0.1)	7	6.9(0.1) ^d	77(3)	1.6(0.2)
	L-NAME	5	n/d	16(7)	n/d	4	n/d	18(4)	n/d	4	n/d	10(5)	n/d
	indomethacin	6	7.3(0.2)	74(7)	4.6(2.2)	-	-	-	-	7	6.8(0.1)	67(3)	4.7(4.1)
14	Control	11	7.7(0.1)	86(2)	1.4(0.2)	4	7.3(0.1) ^c	80(1)	1.0(0.3)	9	7.4(0.1) ^c	82(3)	0.9(0.1)
	L-NAME	7	n/d	13(6)	n/d	4	n/d	7(5)	n/d	4	n/d	25(12)	n/d
	indomethacin	11	7.4(0.1)	76(3)	3.9(1.3)	-	-	-	-	9	6.7(0.3) ^c	84(18)	4.8(1.6)

Table 4.1. Parameters for 2fly CRC in saline and 2fly treated C57 mice in the presence of nonselective inhibitors of NOS and COX. Values are mean (SE), n = mice/ group. Variables were determined by nonlinear regression curve fitting of the averaged 2fly concentration-relaxation responses for each mouse using a four parameter logistic equation. n/d indicates data that could not be fit to equation. -, not tested. 2fly low dose, 2 nmol/kg/min, 2fly high dose, 6 nmol/kg/min; L-NAME, 300 μM; indomethacin, 10 μM. Statistics tests (2 way ANOVA) indicating significant main effects and interactions were followed by Bonferroni post-hoc testing for multiple comparison testing. ^a P<0.001, significant effect of pump. ^b P<0.01, significant effect of time. ^c P<0.05, compared to saline in each group (Bonferroni). ^d P<0.01, compared to saline in each group (Bonferroni). ^e P<0.001, compared to control with the same treatment (Bonferroni).

4.1.2 Acetylcholine Relaxation

Acetylcholine-induced relaxations were measured to determine if there was a change in endothelium-dependent nitric oxide relaxations by PAR₂-AP *in vivo* treatments. Acetylcholine E_{max} values in C57 aortas were attenuated by 16% and 25% after 7 days of HD and 14 days of LD PAR₂-AP treatment, respectively, compared to controls (Table 4.2, Figure 4.2A and B). pD₂ and hill slope values for ACh CRC were not different across all groups. ACh CRC of aortas from chronic PAR₂-AP treated PAR₂^{-/-} were not different than in saline-treated PAR₂-AP (Figure 4.2C and D, Table 4.3). These data indicate endothelium-dependent nitric oxide relaxation was reduced by specific doses and duration of exposure to PAR₂-AP in C57 mice.

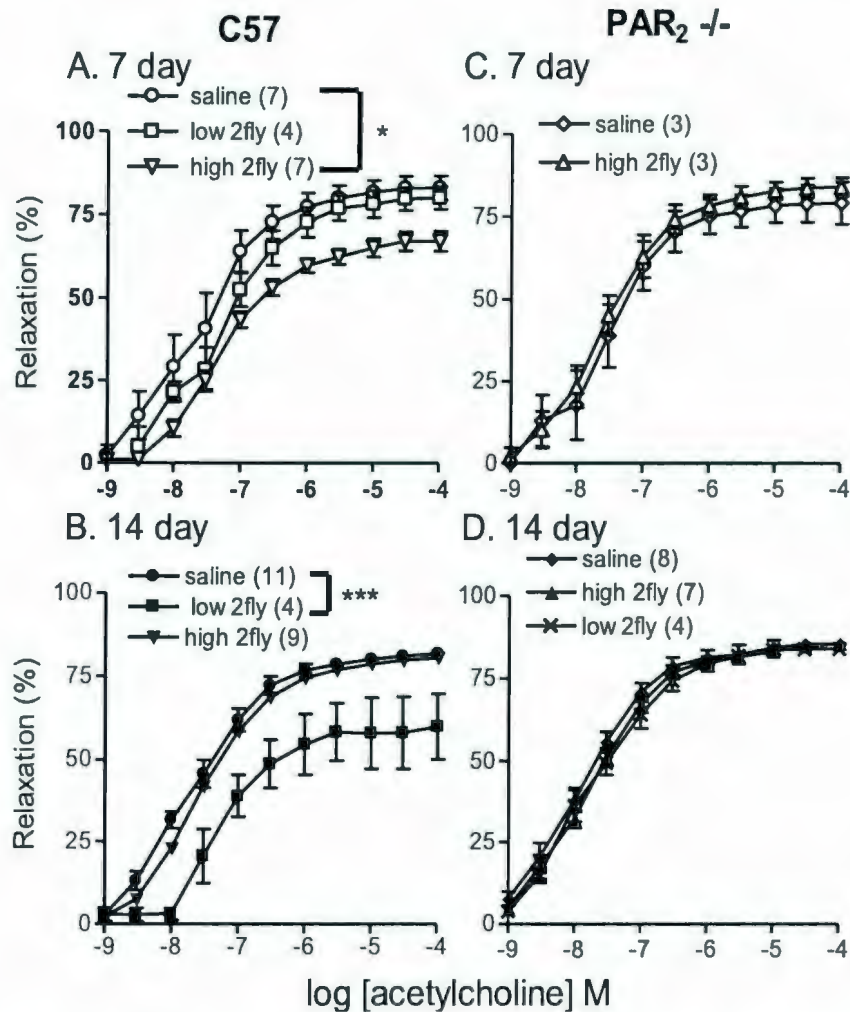


Figure 4.2. Effect of PAR₂-AP s.c. infusions for 7 (A, C) and 14 (B, D) days on acetylcholine-induced relaxations of isolated C57 aortas PAR₂^{-/-} aortas. Mice were implanted with 7 (A, C) and 14 (B, D) day pumps s.c. Isolated aortas were contracted submaximally (50-80%) by U46619 prior to determining relaxation by acetylcholine. Values in parentheses are the number of mice. * P < 0.05 E_{max} , 7 day saline vs. 7 day 2fly high dose and * P < 0.001 E_{max} , 14 day saline vs. 14 day 2fly low dose by 2 way ANOVA, Bonferroni.**

acetylcholine			micro-Osmotic Pump Treatment										
Duration (days)	Artery Treatment	n	Saline			2fly low dose				2fly high dose			
			pD ₂ (M)	E _{max} (%)	Hill Slope	n	pD ₂ (M)	E _{max} ^{a,b} (%)	Hill Slope	n	pD ₂ (M)	E _{max} ^{a,b} (%)	Hill Slope
7	Control	7	7.6(0.2)	81(3)	1.2(0.2)	4	7.3(0.1)	76(3)	0.9(0.1)	7	7.2(0.1)	68(3) ^c	0.9(0.1)
	L-NAME	5	n/d	23(12)	n/d	4	n/d	28(8)	n/d	4	n/d	23(15)	n/d
	Indomethacin	6	7.3(0.1)	69(9)	1.5(0.3)	-	-	-	-	7	6.9(0.2)	66(8)	1.2(0.3)
14	Control	11	7.6(0.1)	81(2)	0.9(0.1)	4	7.2(0.1)	61(9) ^d	1.1(0.2)	9	7.5(0.1)	81(3)	0.9(0.1)
	L-NAME	7	n/d	24(12)	n/d	4	n/d	23(10)	n/d	4	n/d	27(12)	n/d
	Indomethacin	11	7.7(0.4)	72(5)	4.2(2.4)	-	-	-	-	9	7.3(0.2)	78(3)	1.5(0.4)

Table 4.2. Parameters for acetylcholine CRC in saline and 2fly treated C57 mice in the presence of nonselective inhibitors of NOS and COX. Values are mean (SE), n = mice/ group. Variables were determined by nonlinear regression curve fitting of the averaged acetylcholine concentration-relaxation responses for each mouse using a four parameter logistic equation. n/d indicates data that could not be fit to equation. -, not tested. 2fly low dose, 2 nmol/kg/min; 2fly high dose, 6 nmol/kg/min; L-NAME, 300 μM; indomethacin, 10 μM. Statistics tests (2 way ANOVA) indicating significant main effects and interactions were followed by Bonferroni post-hoc testing for multiple comparison testing. ^a P<0.005, significant interaction between pump and time. ^b P<0.01, significant effect of time. ^c P<0.05, compared to saline in same group. ^d P<0.001, compared to saline in same group.

acetylcholine			micro-Osmotic Pump Treatment										
Duration (days)	Artery Treatment	n	Saline			2fly low dose				2fly high dose			
			pD ₂ (M)	E _{max} (%)	Hill Slope	n	pD ₂ (M)	E _{max} (%)	Hill Slope	n	pD ₂ (M)	E _{max} (%)	Hill Slope
7	Control	3	7.5(0.2)	78(6)	1.0(0.2)	-	-	-	-	3	7.6(0.1)	83(3)	1.0(0.1)
	Indomethacin	3	7.2(0.1)	75(1)	1.8(0.2)	-	-	-	-	3	7.6(0.1)	65(20)	3.7(2.7)
14	Control	8	7.9(0.1)	85(2)	0.9(0.1)	4	7.7(0.1)	84(1)	0.81(0.06)	7	7.7(0.1)	84(2)	0.9(0.1)
	Indomethacin	7	7.4(0.3)	68(7)	4.4(2.1)	-	-	-	-	7	7.8(0.3)	76(7)	2.9(1.9)

Table 4.3. Parameters for acetylcholine CRC in saline and 2fly treated PAR₂^{-/-} mice in the presence of nonselective inhibitors of NOS and COX. Values are mean (SE), n = mice/ group. Variables were determined by nonlinear regression curve fitting of the averaged acetylcholine concentration-relaxation responses for each mouse using a four parameter logistic equation. -, not tested. 2fly low dose, 2 nmol/kg/min; 2fly high dose, 6 nmol/kg/min; indomethacin, 10 μM. Statistics tests (2 way ANOVA) indicating significant main effects and interactions were followed by Bonferroni post-hoc testing for multiple comparison testing. No significant differences were found.

4.1.3 Nitroprusside Relaxation

Nitroprusside relaxations were measured to determine if there was a change in endothelium-independent nitric oxide-mediated relaxation by PAR₂-AP treatments. PAR₂-AP treatment *in vivo* caused time and dose dependent effects on nitroprusside CRC of mouse aortas. After 14 days LD PAR₂-AP treatment, nitroprusside E_{max} was attenuated by ~28% compared to C57 controls (Figure 4.3B, Table 4.4). Nitroprusside E_{max} values were not significantly different between HD PAR₂-AP and saline treatments (Table 4.4). pD₂ and hill slopes of nitroprusside CRC were not different among groups (Table 4.4). Nitroprusside CRC in PAR₂^{-/-} were not affected by chronic PAR₂-AP treatment (Figure 4.3C and D, Table 4.5). These data indicate that at 14 day LD PAR₂-AP treatment there was an unexpected decrease in endothelium-independent nitric oxide-mediated relaxation.

4.1.4 A23187 Relaxation

A23187 relaxations were measured to determine if there was a change in receptor-independent endothelium-dependent nitric oxide relaxations by PAR₂-AP treatments. Relaxations mediated by A23187 were not found to differ between any of the groups (Figure 4.4; compare 1 μM responses for saline versus 2fly-treated, Student's t-test, P>0.05). We noted that tissue responses observed at 3 μM A23187 were highly variable. The solubility of 3 μM A23187 was poor, and thus, the relaxation data obtained at the highest concentrations may not be reliable. No differences in receptor-independent endothelium-dependent nitric oxide relaxation were found.

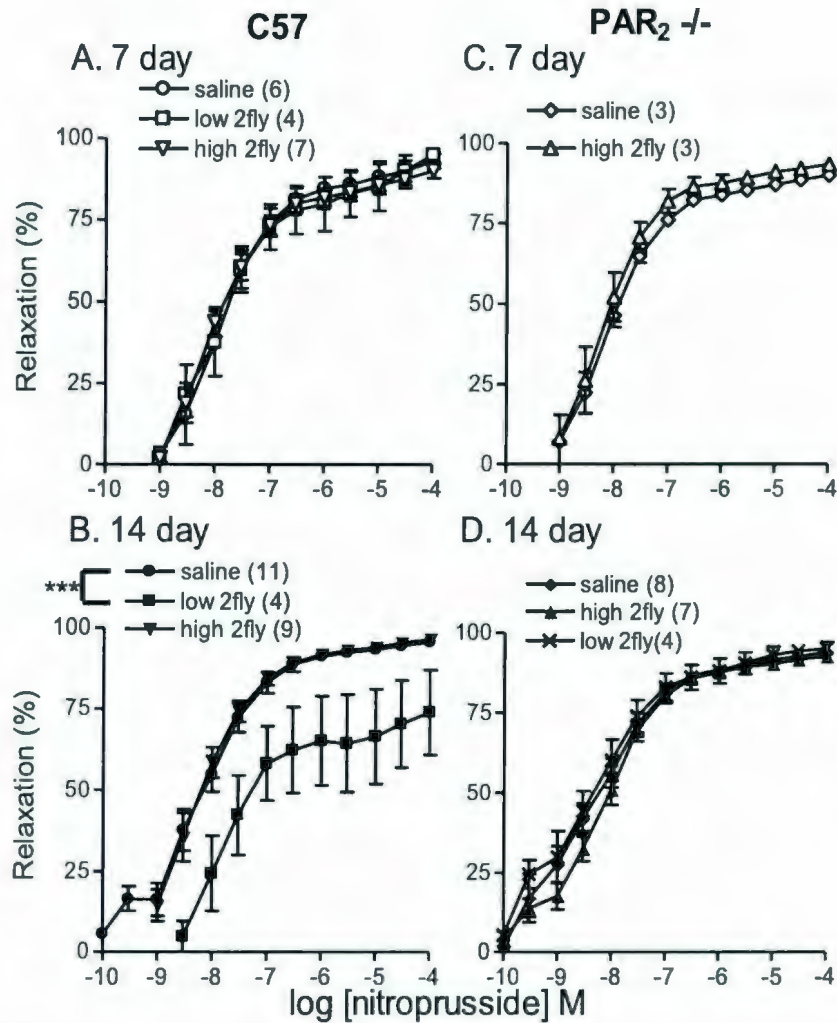


Figure 4.3. Effect of PAR₂-AP s.c. infusions for 7 (A, C) and 14 (B, D) days on nitroprusside-induced relaxations of isolated C57 and PAR₂^{-/-} aortas. Mice were implanted with 7 (A, C) and 14 (B, D) day pumps s.c. Isolated aortas were contracted submaximally (50-80%) by U46619 prior to determining relaxation by nitroprusside. Values in parentheses are the number of mice. *** P<0.001 E_{max}, 14 day saline vs. 14 day low dose 2fly, by 2 way ANOVA, Bonferroni.

nitroprusside			micro-Osmotic Pump Treatment										
Duration (days)	Artery Treatment	n	Saline			2fly low dose				2fly high dose			
			pD ₂ (M)	E _{max} (%)	Hill Slope	n	pD ₂ (M)	E _{max} ^{a,b} (%)	Hill Slope	n	pD ₂ (M)	E _{max} ^{a,b} (%)	Hill Slope
7	Control	6	7.8(0.2)	93(2)	0.9(0.1)	4	7.8(0.2)	87(6)	0.9(0.1)	7	7.8(0.1)	90(2)	0.9(0.1)
	L-NAME	5	8.1(0.2)	92(4)	1.1(0.2)	4	8.3(0.1)	94(2)	0.9(0.1)	4	7.9(0.1)	91(3)	0.8(0.1)
	Indomethacin	6	7.6(0.8)	90(3)	0.9(0.2)	-	-	-	-	7	8.4(0.1)	83(7)	2.5(1.7)
14	Control	11	8.2(0.1)	93(1)	1.0(0.1)	4	7.7(0.1)	67(14) ^c	1.5(0.3)	9	8.2(0.1)	96(1)	0.8(0.1)
	L-NAME	7	7.9(0.2)	91(2)	1.0(0.1)	4	8.2(0.2)	92(1)	1.0(0.1)	4	7.0(0.2)	93(1)	1.1(0.2)
	Indomethacin	11	8.0(0.2)	84(4)	2.7(1.0)	-	-	-	-	7	8.4(0.1)	91(1)	1.6(0.5)

Table 4.4. Parameters for nitroprusside CRC in saline and 2fly treated C57 mice in the presence of nonselective

inhibitors of NOS and COX. Values are mean (SE), n = mice/ group. Variables were determined by nonlinear regression curve fitting of the averaged nitroprusside concentration-relaxation responses for each mouse using a four parameter logistic equation. n/d indicates data that could not be fit to equation. -, not tested. 2fly low dose, 2 nmol/kg/min; 2fly high dose, 6 nmol/kg/min; L-NAME, 300 μM; indomethacin, 10 μM. Statistics tests (2 way ANOVA) indicating significant main effects and interactions were followed by Bonferroni post-hoc testing for multiple comparison testing.^a P<0.05, significant interaction between pump and time. ^b P<0.001, significant effect of pump. ^c P<0.001, compared to saline in same group (Bonferroni).

nitroprusside				micro-Osmotic Pump Treatment									
Duration (days)	Artery Treatment	n	Saline			2fly low dose				2fly high dose			
			pD ₂	E _{max} (%)	Hill Slope	n	pD ₂	E _{max} (%)	Hill Slope	n	pD ₂	E _{max} (%)	Hill Slope
7	Control	3	8.0(0.1)	87(1)	1.0(0.18)	-	-	-	-	3	8.1(0.2)	90(1)	1.0(0.1)
	Indomethacin	3	7.9(0.2)	89(7)	0.6(0.2)	-	-	-	-	3	7.3(0.9)	92(4)	3.4(2.1)
14	Control	8	8.4(0.1)	92(1)	0.7(0.1)	4	8.5(0.2)	94(2)	0.6(0.1)	7	8.2(0.1)	91(1)	0.8(0.1)
	Indomethacin	7	8.1(0.1)	85(2)	1.0(0.3)	-	-	-	-	7	8.1(0.2)	82(3)	0.9(0.1)

Table 4.5. Parameters for nitroprusside CRC in saline and 2fly treated PAR₂^{-/-} mice in the presence of nonselective inhibitors of NOS and COX. Values are mean (SE), n = mice/ group. Variables were determined by nonlinear regression curve fitting of the averaged nitroprusside concentration-relaxation responses for each mouse using a four parameter logistic equation. n/d indicates data that could not be fit to equation. -, not tested. 2fly low dose, 2 nmol/kg/min; 2fly high dose, 6 nmol/kg/min; indomethacin, 10 μM. Statistics tests (2 way ANOVA) indicating significant main effects and interactions were followed by Bonferroni post-hoc testing for multiple comparison testing. No significant differences were found.

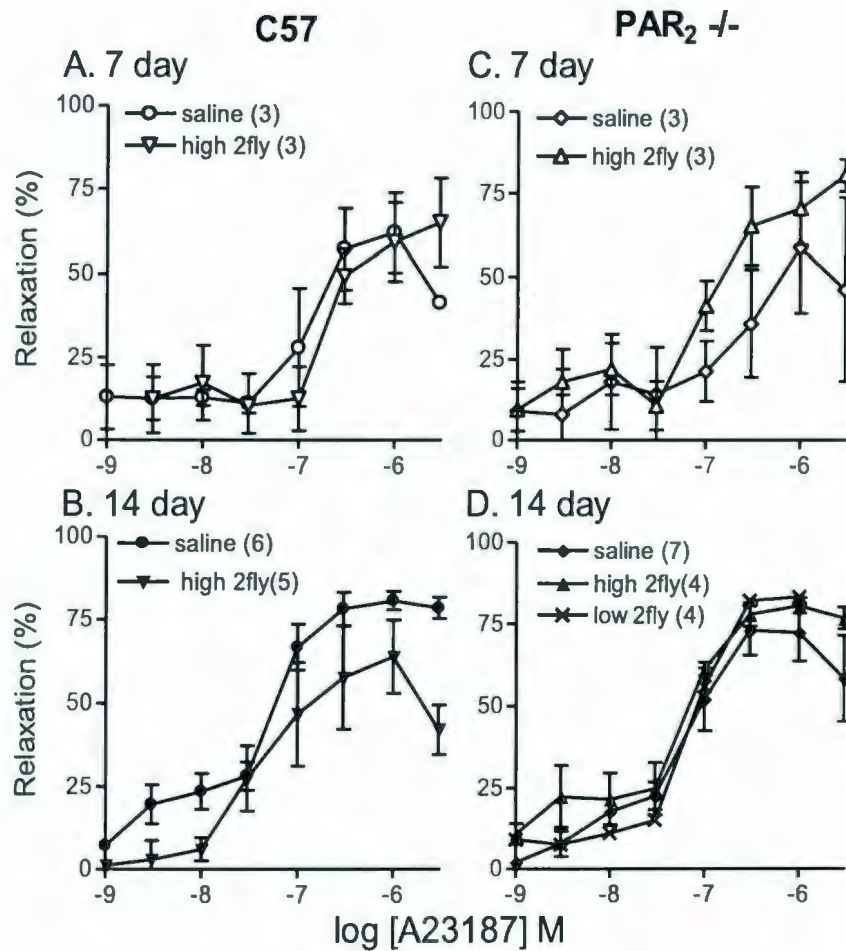


Figure 4.4. Effect of PAR₂-AP s.c. infusions for 7 (A, C) and 14 (B, D) days on A23187-induced relaxations of isolated C57 and PAR₂^{-/-} aortas. Mice were implanted with 7 (A, C) and 14 (B, D) day pumps s.c. Isolated aortas were contracted submaximally (50-80%) by U46619 prior to determining relaxation by A23187. Values in parentheses are the number of mice. The maximal relaxations did not differ amongst groups A, B, and C (Students t-test) and D (one way ANOVA).

4.1.5 Intact versus denuded endothelium

To describe the agonists' dependencies on intact endothelium, aortas were subjected to endothelial cell denudation by rotating the aortas on wires in the myograph chambers. ACh, 2fly, and A23187 were found to be all endothelium-dependent as they caused minor if any relaxation in the denuded aortas of C57 or PAR₂^{-/-} (Figures 4.5 and 4.6). Nitroprusside did elicit relaxation of denuded aorta, albeit reduced, in both C57 and PAR₂^{-/-}, indicating relaxation was independent of endothelium (Figures 4.5 and 4.6). The agonists showed specificity to endothelium as expected.

4.1.6 Effect of eNOS and COX inhibition on vasodilators

To determine underlying mechanisms of NO-dependent drugs the effect of inhibition of eNOS and cyclooxygenases were measured using L-NAME and indomethacin respectively. L-NAME dramatically inhibited relaxation by 2fly (Table 4.1) and acetylcholine (Table 4.2) but had no effect on nitroprusside CRC (Table 4.4) in either treatment group. E_{max} values for 2fly and acetylcholine (Tables 4.1 and 4.2) CRC in the presence of L-NAME were significantly reduced compared to controls (P<0.001, 2 way ANOVA). E_{max}, pD₂, and hill slope of nitroprusside CRC in the presence of L-NAME (Tables 4.4) were not different than untreated aortas (P>0.05, 2 way ANOVA). Indomethacin pretreatment of aortas caused a rightward shift as measured by a reduction in pD₂ values for 2fly relaxation in C57 2fly HD 14 day treated mice as illustrated in Figure 4.7D and Table 4.1 (P<0.001). In summary, inhibition of eNOS caused expected reductions in relaxation while blocking cyclooxygenases caused a rightward shift.

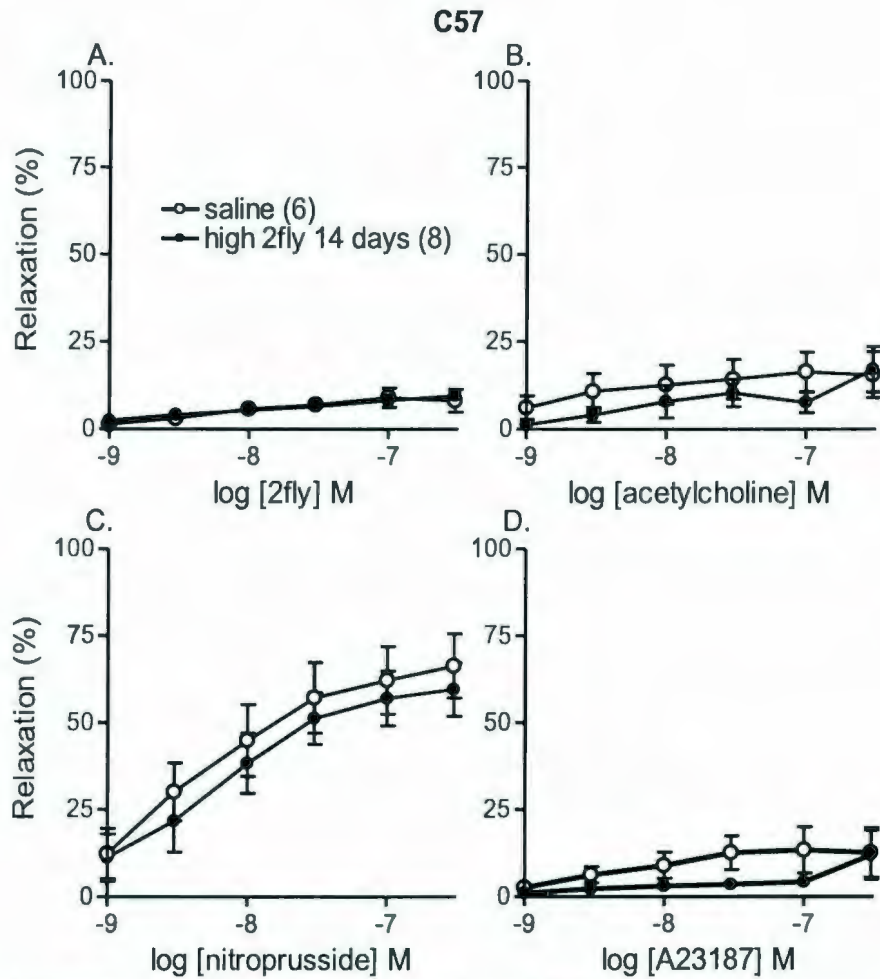


Figure 4.5. Effect of endothelium denudation of C57 aortas on 2fly-, acetylcholine-, nitroprusside- and A23187-induced relaxations. The endothelium was removed from aortas by rotating them around hooks prior to setting ring tension. Aortas were then contracted by U46619 and then exposed to 2fly, acetylcholine, nitroprusside and A23187. Values in parentheses are the number of mice. All data points for 2fly, ACh, and A23187 (A, B, D), but not nitroprusside (C) were not different than zero (one sample Students t-test). In C, saline vs. 2fly, the maximal response was not significantly different (Students t-test).

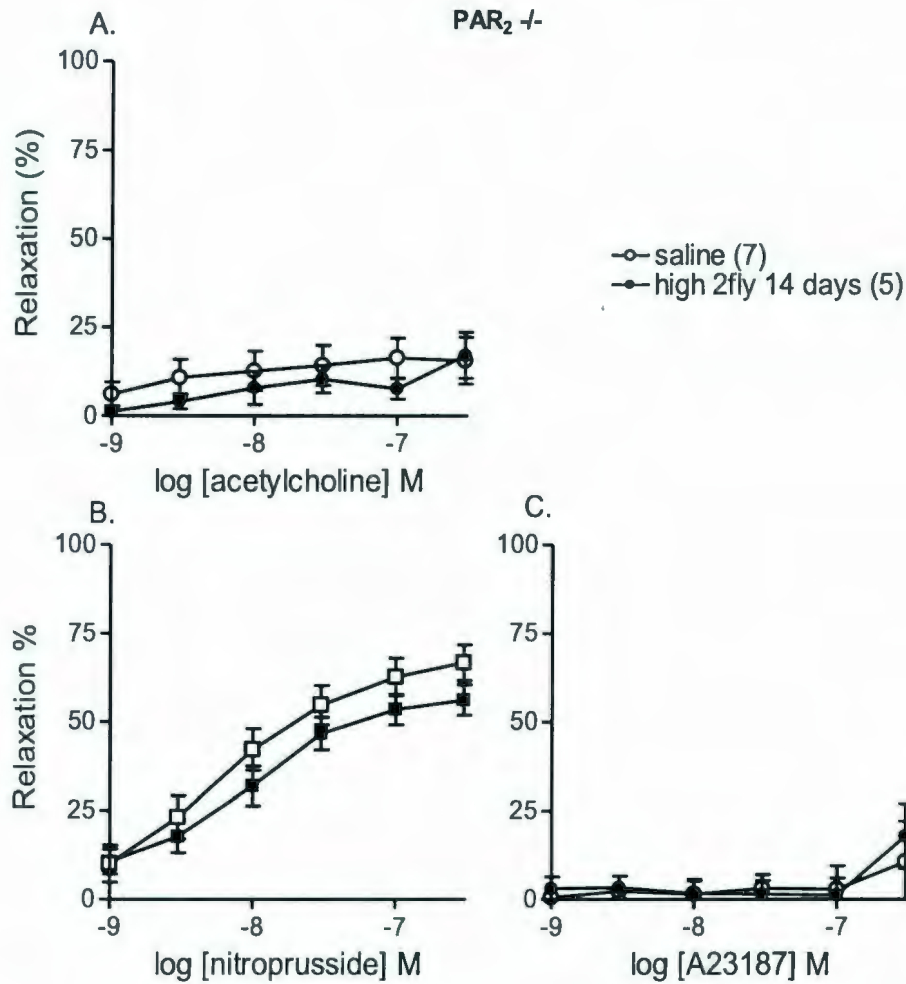


Figure 4.6. Effect of endothelium denudation of PAR₂^{-/-} aortas on acetylcholine-, nitroprusside- and A23187-induced relaxations. The endothelium was removed from aortas by rotating them around hooks prior to setting resting tension. Aortas were contracted by U46619 and then exposed to acetylcholine, nitroprusside, and A23187. Values in parentheses are the number of mice. All data points for ACh and A23187 (A and C), but not nitroprusside (B) were not different than zero (one sample Students t-test). In B, saline vs. 2fly, the maximal response was not significantly different (Students t-test).

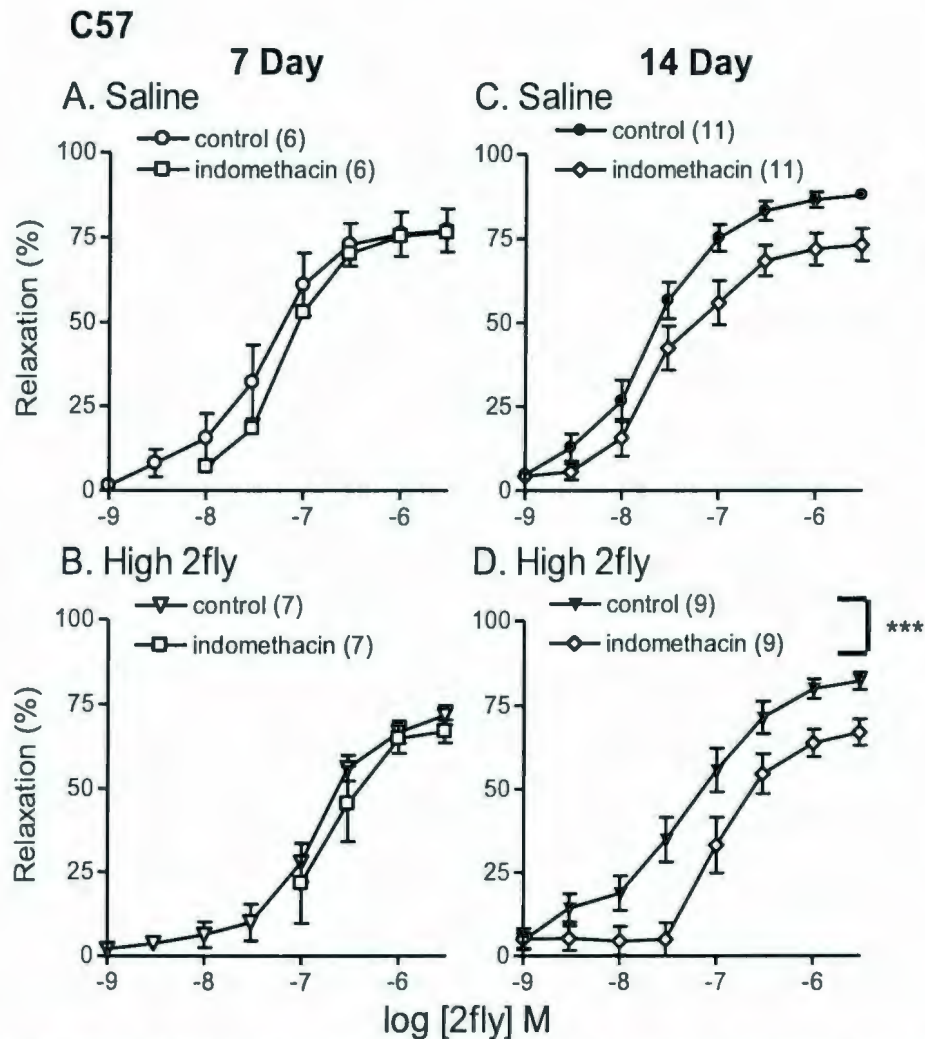


Figure 4.7. Effect of indomethacin on 2fly-induced relaxations of aortas from PAR₂-AP treated C57. Mice were treated with saline (A, C) or high dose 2fly (B, D) s.c. for 7 (A, B) or 14 (C, D) days. Isolated aortas were pretreated with indomethacin (10 μ M) for 15 min prior to submaximal contraction by U46619 (50-80 %) and then exposing to 2fly. Values in parentheses are the number of mice. *** $P < 0.001$ pD₂, 14 day 2fly control vs. 14 day 2fly indomethacin, by 2 way ANOVA, Bonferroni.

4.2 Chronic PAR₂-AP treatment effect on expressions of COX isoforms 1 and 2, eNOS and sGC in mouse aortas

Measurement of COX isoforms, eNOS, and sGC in aortic rings was performed to identify if the changes in aortic functional responses were due in part to changes in protein expression of components involved in the relaxation mechanism.

Immunoreactivity indicative of COX-1, COX-2, eNOS and sGC were detected in aortic protein from both saline and PAR₂-AP treated animals (Figure 4.8B, and 4.9C).

Densitometric analyses of target bands indicated the relative expression of COX-1 and COX-2 did not differ between saline-treated and PAR₂-AP treated C57 aortas (Figure 4.8A). Expression of sGC and eNOS were not significantly different between saline and PAR₂-AP treatments (Figure 4.9A) as well as between strains (Figure 4.9B). These data indicate the change seen in aortic responsiveness did not have a corresponding change in these target proteins between groups.

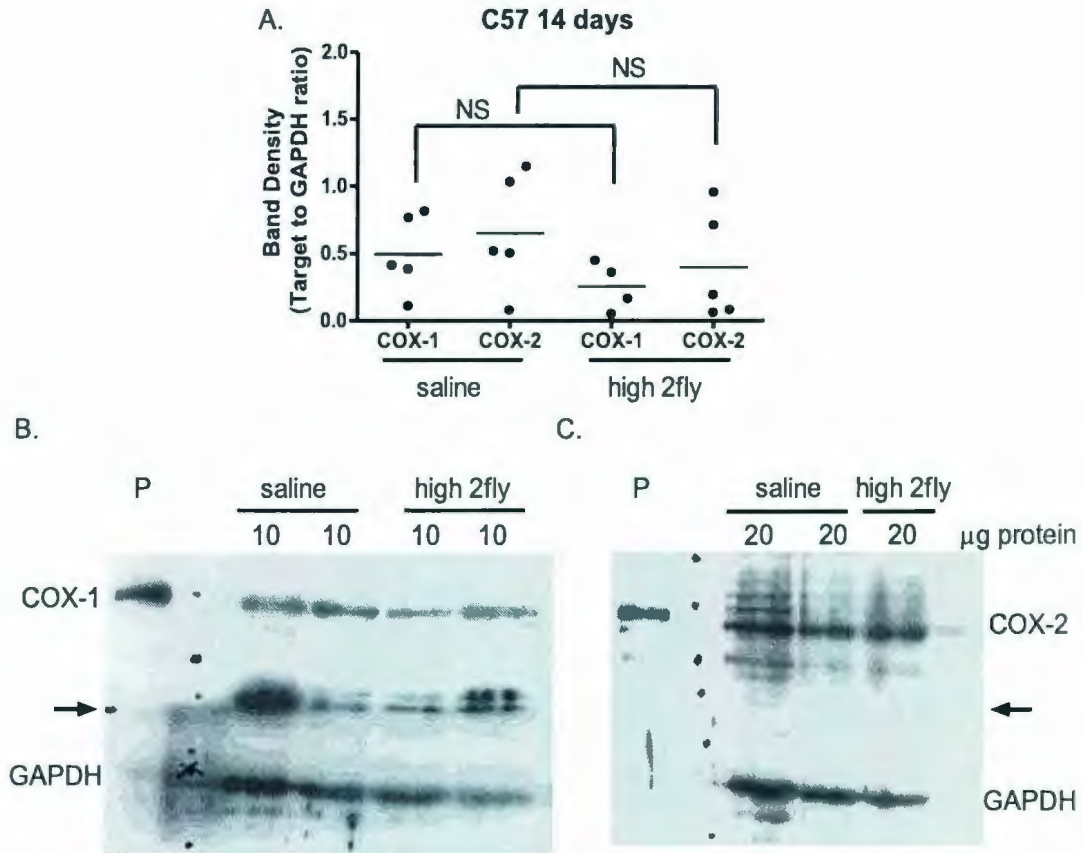


Figure 4.8. Expression of COX-1 and COX-2 proteins in aortas of C57 mice infused s.c. with saline or high dose 2fly for 14 days. (A) Summary of densitometry of COX-1 and COX-2 in C57 mice compared to GAPDH from saline and high dose 2fly treated animals. Each symbol indicates an independent sample. Representative western blots for COX-1 (B) and COX-2 (C). P, indicates positive control sample (0.5 μ g vas deferens protein). Arrows represent where the membranes were cut to immunoblot for GAPDH. $P > 0.05$, saline vs. high 2fly, Student's t-test.

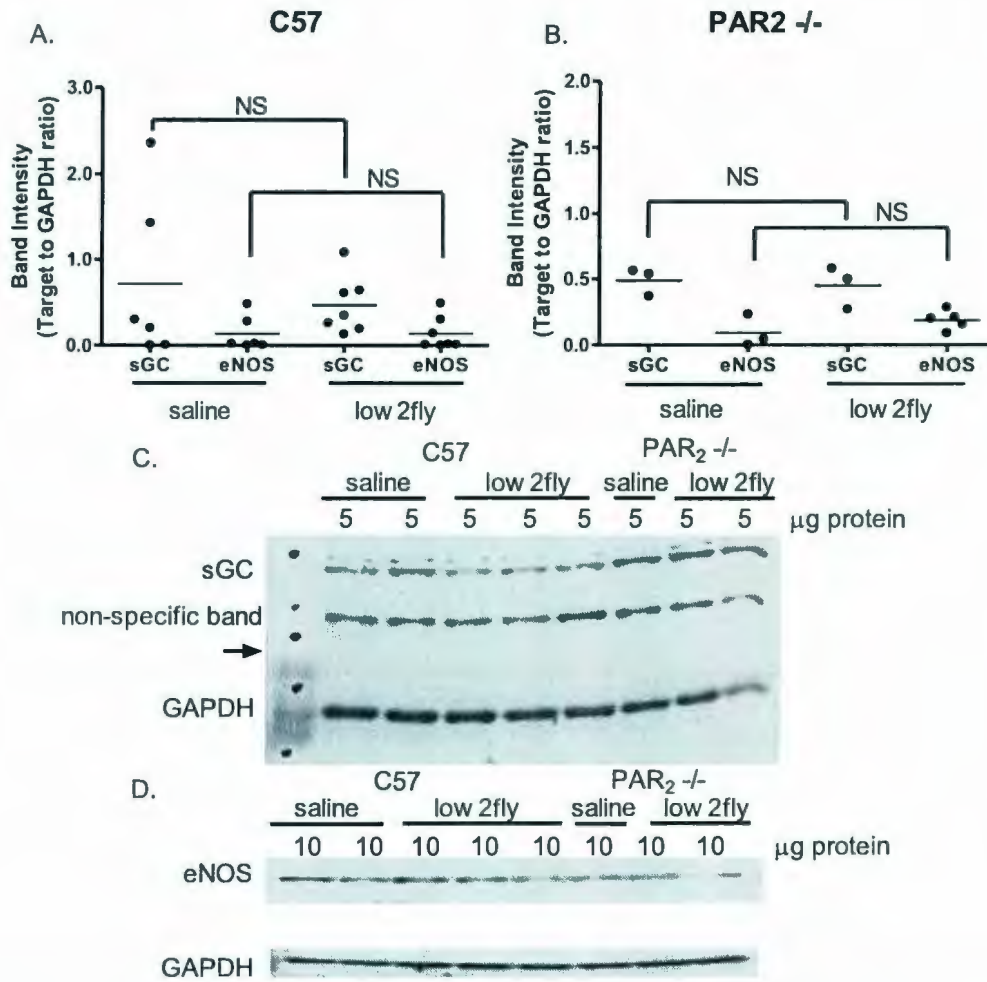


Figure 4.9. Expression of sGC and eNOS protein in aortas of C57 and PAR₂^{-/-} mice infused s.c. with saline or low dose 2fly for 14 days. Summary of densitometry of sGC and eNOS in C57 (A) and PAR₂^{-/-} (B) mice compared to GAPDH from saline and low dose 2fly treated animals. Each symbol indicates an independent sample. Representative western blots for sGC (C) and eNOS (D). Arrows represent where the membranes were cut. P>0.05, saline vs. low 2fly, Student's t-test.

4.3 Characteristics of SAM11 “anti-PAR₂” antibody immunofluorescence in mouse aortas

PAR₂ immunofluorescence experiments were performed to determine if the changes in aortic function to 2fly was due to a change in the amount of receptor present in the vessel wall. SAM11 antibody staining of aortas from both C57 and PAR₂^{-/-} was detected by immunofluorescence using confocal microscopy (Upper panels of Figures 4.10 and 4.11). Qualitatively the images did not differ (Upper panels of Figures 4.10 and 4.11). Quantifying the pixel density distribution across the aortic wall (from lumen to exterior) indicated no obvious differences in the fluorescence signal pattern for either strain or treatment groups (Bottom panels of Figure 4.10 and 4.11). From the immunostaining procedure used we were unable to measure any differences in PAR₂ tissue distribution.

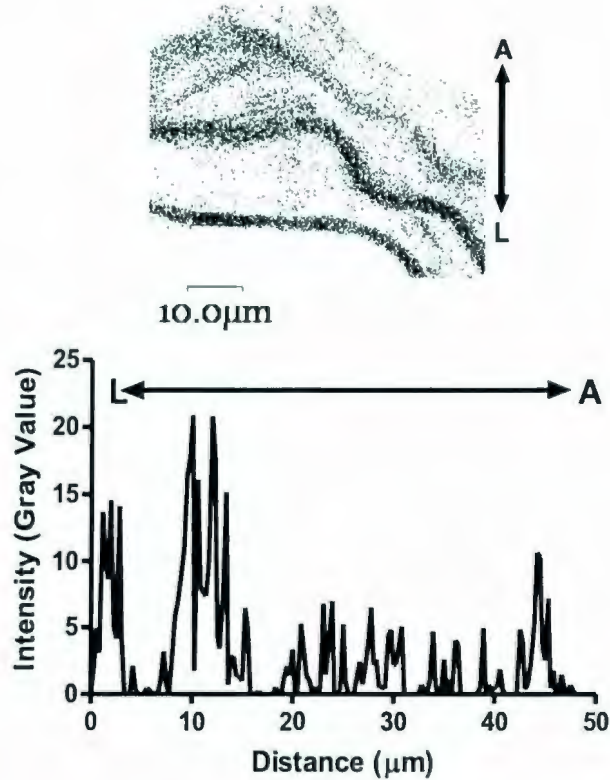


Figure 4.10. Immunofluorescence of SAM11 antibody staining in C57 aortas. Image (upper panel; 1 μm confocal plane steps) from frozen section of aorta (8 micron thick) incubated with primary antibody SAM11 (anti-PAR₂) followed by secondary antibody FITC. Shown above is C57 2fly treated HD, SAM11, dilution 1:100 and FITC, dilution 1:100. Lower panel is a representative line scan of pixel intensity across the aortic wall using ImageJ software. The acquired colour confocal image was modified for reproduction purposes only and shown as above. Using Adobe Professional software the acquired image was grayscaled, inverted and the contrast was increased. In the original image black (empty) background and green immunofluorescence are reproduced as white and black, respectively. L, lumen and A, adventitia.

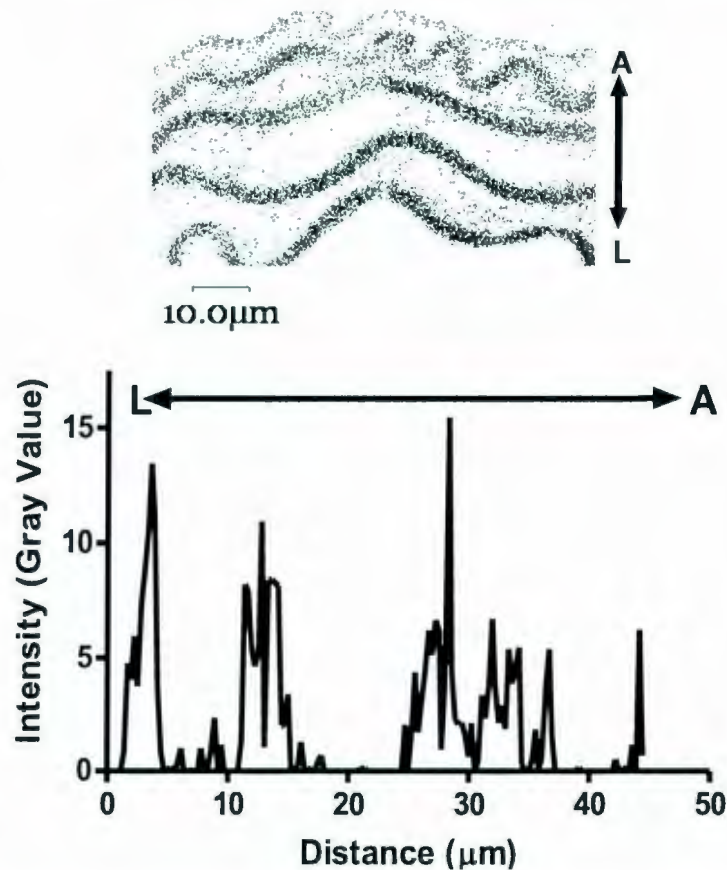


Figure 4.11. Immunofluorescence of SAM11 antibody staining in $PAR_2^{-/-}$ aortas.

Image (upper panel; 1 μ m confocal plane steps) from frozen section of aorta (8 micron thick) incubated with primary antibody SAM11 (anti- PAR_2) followed by secondary antibody FITC. Shown above is $PAR_2^{-/-}$ control, SAM11, dilution 1:100 and FITC, dilution 1:100. Lower panel is a representative line scan of pixel intensity across the aortic wall using ImageJ software. Using Adobe Professional software the acquired color confocal image was grayscale, inverted and the contrast was increased. In the original image black (empty) background and green immunofluorescence are reproduced as white and black, respectively. L, lumen and A, adventitia.

4.4 Blood pressure, heart rate and locomotor activity

Blood pressures, heart rate and locomotor activity were measured to determine if chronic high dose PAR₂-AP lowered blood pressure in mice. First, an analysis of the baseline (i.e. prior to treatments) telemetry data was performed to see if the blood pressures were different between PAR₂^{-/-} and C57 mice as described previously (McGuire *et al.*, 2008). The averaged 24 h baseline data for each variable, mean arterial pressure (MAP), systolic arterial pressure (SAP), diastolic arterial pressure (DAP), heart rate (HR), pulse pressure (PP), and locomotor activity, are summarized in table 4.6. The MAP and SAP in PAR₂^{-/-} were significantly higher than in C57 mice by ~7 mmHg and ~8 mmHg, respectively (P<0.05). Heart rates were about 60 beats min⁻¹ higher in PAR₂^{-/-} than in C57 mice (P<0.05). A ~7% decrease in activity was measured in PAR₂^{-/-} compared to C57 was also found (P<0.01). The higher baseline systolic values in PAR₂^{-/-} were reported previously (McGuire *et al.*, 2008), but both the higher heart rate and lowered activity had not been observed.

During the infusion period with PAR₂-AP, the averaged 24 h MAP, SAP, DAP, PP, HR and locomotor activity values were not found to be significantly different between most of the groups (P>0.05, Figure 4.12). The exception was a ~15% (100 beats min⁻¹) lowered heart rate in C57 controls compared to C57 14 day HD PAR₂-AP (P<0.05 to P<0.001 as indicated for individual treatment days; Figure 4.12D). Overall, there was no change in the mean values of the blood pressures values recorded between the treatment groups.

Given the small sample sizes in each of the groups during the treatment periods, we prepared an alternative analyses of data that would be expected to reduce the variation within groups for statistics testing. This analysis of the hemodynamic variables and locomotor activity was comprised of calculating the dependent variable change relative to the baseline periods within each group. Based on this analyses, significant decreases in systolic and pulse pressures were observed in C57 mice which were administered high dose 2fly and these pressure changes were significantly different compared to saline-treated C57 ($P < 0.05$ to $P < 0.001$ for different days, Figure 4.13). There were no differences in variables between $PAR_2^{-/-}$ treatment groups (Figure 4.13). Systolic blood pressure was lowered ~ 7 mmHg and pulse pressure lowered ~ 4 mmHg in 2fly HD C57 compared to saline-treated C57 (Figure 4.13B and 4.13F). The other parameters were not significantly different between saline and 2fly administered mice of either strain. Therefore, blood pressure changes relative to the baseline periods were different between PAR_2 -AP and saline treatments in C57, but not $PAR_2^{-/-}$ mice.

24 hour mean variable	C57 n=6	PAR ₂ ^{-/-} n=8	Ratio PAR2 ^{-/-} to C57
MAP (mmHg)	101.3 (2.5)	108.3 (1.5)*	1.07
SAP (mmHg)	113.5 (3.0)	122 (1.6)*	1.07
DAP (mmHg)	87.9 (2.1)	93.5 (1.9)	1.06
HR (beats min ⁻¹)	534 (24)	593 (7)*	1.11
Activity (%)	41.5 (1.3)	33.6 (1.9)**	0.81
PP (mmHg)	25.6 (2.3)	28.4 (2.0)	1.11
Offset (mmHg)	4.2 (0.8)	4.0 (0.5)	n/a

Table 4.6. 24 h baseline hemodynamics and locomotor activity data from C57 and PAR₂^{-/-} mice. Data were recorded for baseline period for 2-4 days prior to pump implants. Values are mean (SE), n = mice/ group. Offset values indicate the calibrated value measured from implanted telemeters after surgery at 0 mmHg. n/a indicates that a ratio was not applicable for offset values. Pairwise comparisons of variables were made by Student's t-test for unpaired data. * P<0.05 compared to C57. ** P<0.01 compared to C57.

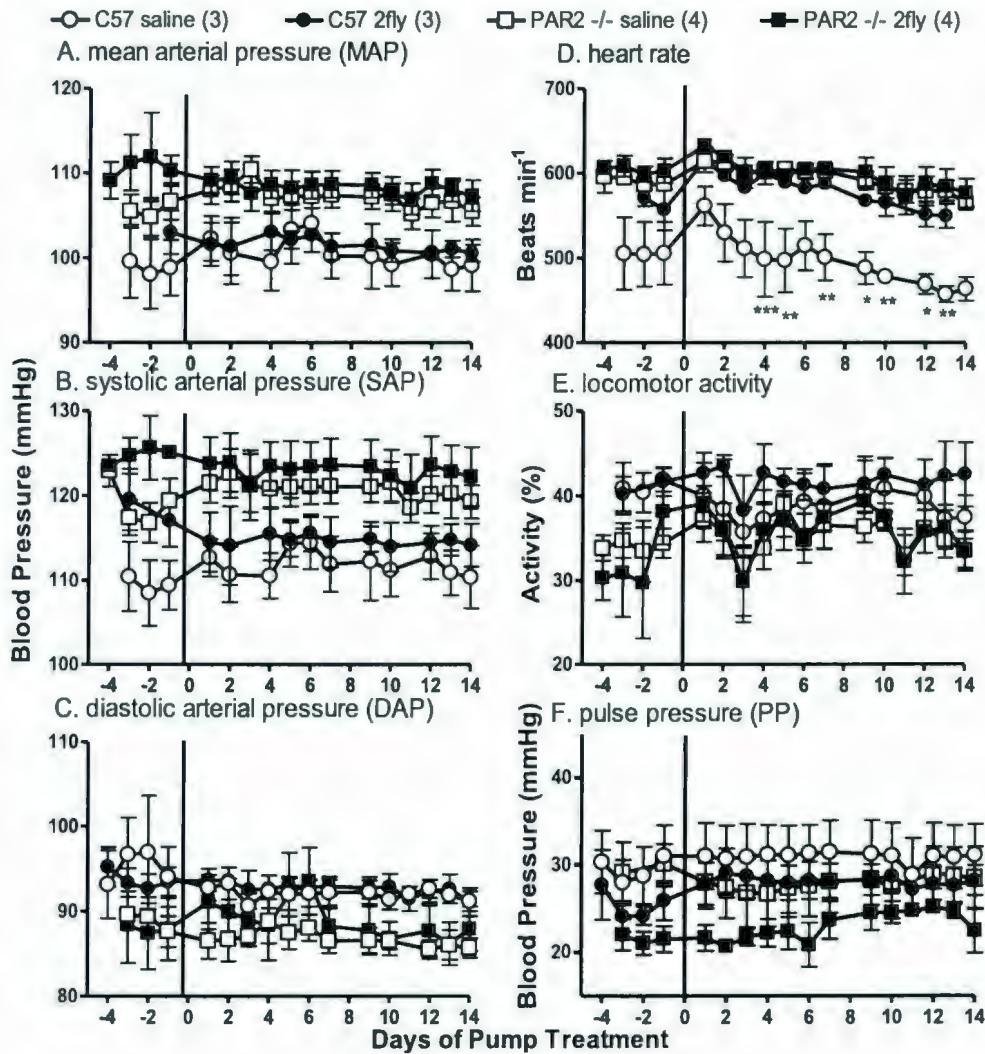


Figure 4.12. Mean 24 h hemodynamics and locomotor activity in C57 and PAR₂^{-/-} during a 4 day baseline period and 14 days treatment with high dose s.c. administered 2fly. Mice were implanted with radiotelemeters 10 days prior to recording baseline (day -4 to -1), pump implant (day 0), and 14 days treatment. Parentheses, number of mice. 24 h averages of MAP, SAP, DAP, HR, activity and PP. * P<0.05, ** P<0.01, * P<0.001, C57 saline vs. C57 high dose 2fly, 2 way ANOVA, Bonferroni.**

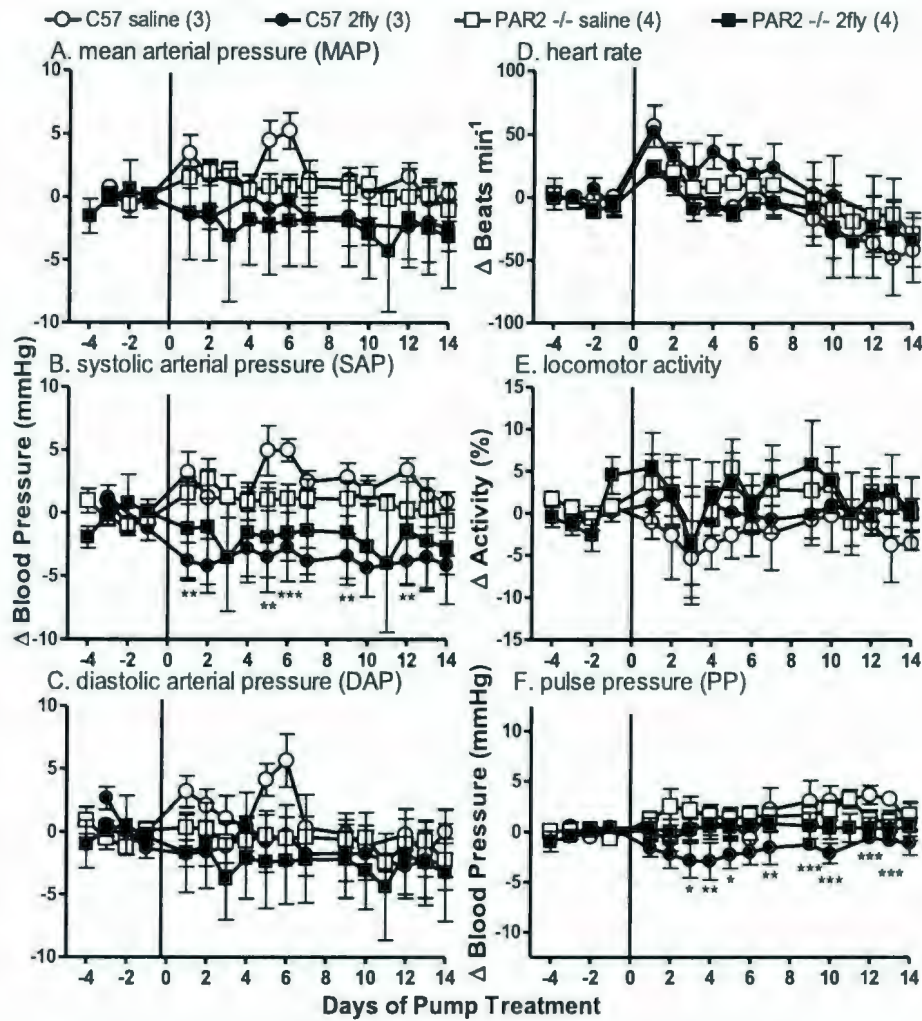


Figure 4.13. Changes in 24 h mean hemodynamic and locomotor activities relative to baseline for C57 and PAR₂^{-/-} during 14 days treatments with high dose s.c. administered 2fly. Mice were implanted with radiotelemeters 10 days prior to recording baseline (day -4 to -1), pump implant (day 0), and 14 days HD PAR₂-AP treatment. Parentheses, number of mice recorded. 24 h averages of change in MAP, SAP, DAP, beats min⁻¹, activity % and PP. * P < 0.05, ** P < 0.01, C57 saline vs. C57 high dose 2fly, 2 way ANOVA, Bonferroni.

Chapter 5: Discussion

5.1 General Findings

We found that chronic *in vivo* administration of the PAR₂ agonist 2fly caused endothelial dysfunction in mouse aortas. This dysfunction was characterized by an attenuation of the maximum relaxations by acetylcholine that occurred in C57, but not in PAR₂^{-/-} mice. This dysfunction in aortas was dose- and time-dependent given that it was observed in 7 day HD 2fly, and 14 day LD 2fly treatments. We found the effectiveness of PAR₂-AP 2fly and endothelium-independent vasodilator nitroprusside were reduced in C57 after PAR₂-AP treatments. Rightward shifts of 2fly CRC were caused by 7 and 14 days of LD and HD 2fly, respectively. Similarly, the reduced maximal effectiveness of nitroprusside was observed in the 14 day LD 2fly treatment group. Calcium ionophore A23187 effectiveness was not affected by the PAR₂-AP treatments. Together these data indicate that PAR₂-AP dysfunction was not restricted to endothelium-dependent relaxation and included endothelium-independent responses to NO.

To assess the effects of PAR₂-AP treatments *in vivo* on the vascular smooth muscle signaling pathways of each agonist, we tested the same agonists activities in the presence of inhibitors of eNOS (L-NAME) or cyclooxygenases (indomethacin). Inhibition of eNOS abolished PAR₂-AP and acetylcholine-induced relaxations of aortas as expected in control C57 (Al-ani *et al.*, 1995; Chataigneau *et al.*, 1999) as well as in PAR₂-AP treated C57. Inhibition of eNOS did not affect nitroprusside-induced relaxations. Inhibition of cyclooxygenases did not have significant effects on acetylcholine- or

nitroprusside-induced relaxations, but did cause a rightward shift in 2fly-induced relaxations of aortas from 14 day HD 2fly C57. This rightward shift may have been the result of some COX activity present at 14 days that aided in relaxation of vessels, and thus, when inhibited a higher concentration of 2fly was needed to achieve the same relaxation. These data indicated that although NOS inhibition was sufficient to inhibit PAR₂-AP induced relaxations, de novo COX activities may have been a supplementary (not critical) relaxation mechanism for PAR₂-AP after 14 day HD 2fly.

An increased expression of COX in aortas of the 14 day HD C57 could have potentially explained the inhibitory effects of indomethacin on 2fly-induced relaxations. However, we found that protein expression of COX-1 and COX-2 were not significantly different between treatment groups in C57 and PAR₂^{-/-}. A decreased concentration of eNOS and sGC could have explained the attenuation of ACh- and nitroprusside-induced relaxations, respectively, but we found there were no significant differences between aortas of PAR₂-AP treated and saline-treated C57. We attempted to assess the expression levels and localization of PAR₂ by labeling sections of frozen aortas with the antibody SAM11, which was raised against the N-terminus of human PAR₂. A potential change in receptor distribution would have been a potential mechanism to explain the attenuated 2fly-induced relaxations of aortas from PAR₂-AP treated C57. However, under the conditions and procedures employed, specific immunofluorescence could not be attributed to PAR₂ receptor expression; i.e. immunofluorescence was detected in PAR₂^{-/-}. While western blot data were able to exclude decreased expression in target protein

expressions of COX-1, COX-2, eNOS and sGC as possible mechanisms, the specific mechanisms causing the attenuated agonist-induced relaxations of aortas remain undetermined.

With regards to measurement of blood pressures, we found that chronic *in vivo* administered 2fly caused mild hypotension in C57 mice. This interpretation of data is supported by our finding of a significant lowering of systolic and pulse pressures as characterized by a change in these variables relative to baseline averages between saline-treated and 2fly high dose treated C57. The absolute blood pressure values that were measured directly did not clearly show any differences between the groups during the treatment periods.

5.2 Effects of administering chronic s.c. PAR₂-AP on mouse aortas *in vitro*

Our study created a novel model of endothelium dysfunction by chronically administering PAR₂-AP *in vivo*. This model is different than endothelial dysfunction models used by other researchers which measure endothelium dysfunction in many different rodent models of disease as well as in human patients (in rodents: Cameron and Cotter, 1992; Dohi *et al.*, 1991; Luscher, 1988; Luscher, 1989; Rajagopalan *et al.*, 1996; Tesfamariam *et al.*, 1989; Viridis *et al.*, 2003 and in humans: Cox *et al.*, 1989; Endemann and Schiffrin, 2004; Perticone *et al.*, 2001; Schachinger *et al.*, 2000).

In our study, acetylcholine-induced relaxation was reduced in a time- and dose-dependent manner; specifically at 7 day HD 2fly and 14 day LD 2fly in C57 mice. The lack of attenuated ACh responses after 7 days LD 2fly C57 may indicate the time effect is

related to an accumulated dose of PAR₂-AP, which was reached earlier by high dose infusions. After 14 day HD 2fly, there was still a decrease in sensitivity to 2fly relative to saline-treated C57 aortas while ACh- and A23187-induced relaxations were not significantly different. This would be consistent with an interpretation that HD PAR₂-AP desensitizes PAR₂ *in vivo*, which leads to a loss of the attenuating action on ACh- and nitroprusside-induced relaxations, and thus, resembles PAR₂-AP treated PAR₂^{-/-}. It was not possible to distinguish between PAR₂ receptor desensitization (e.g. internalization) and a potential tachyphylaxis of a downstream signal causing endothelial dysfunction.

Nitroprusside-induced relaxations of aortas were reduced in 14 day LD 2fly C57 aortas. We could not attribute a decrease in sGC to the effects of *in vivo* PAR₂-AP. A deficit at the vascular smooth muscle level such as increased levels of oxidative stress, which quenches NO and thus, reduces NO bioavailability, could potentially explain both the attenuated nitroprusside- and ACh-induced relaxations of aortas in PAR₂-AP treated C57. Since the 2fly-induced relaxations of aortas of 14 day HD 2fly C57 after treatment were sensitive to indomethacin, an increased level of COX could be proposed as a source of supplementary vasodilator prostanoids (e.g. prostaglandin I₂). We did not find a significant difference in content of COX-1 or COX-2 in total aortic protein between treatments. However, our approach to assay whole aortic proteins would not resolve the differential over expression of COX isoforms in a cell-type specific pattern: i.e. vascular smooth muscle cells protein variation in COX expression may overshadow significant small differences in expression in endothelial cells. It is possible that indomethacin had

an off-target effect that affected 2fly-induced relaxations, but it was specific to only one treatment group. It would be worthwhile for future studies to examine the effects of reactive oxygen scavengers and selective COX-1, and COX-2 inhibitors on aortas from low dose PAR₂-AP treated C57 at 14 days.

5.3 Effect of administering chronic s.c. PAR₂-AP on hemodynamics *in vivo*

Our laboratory is the first to study the effects of chronic administered PAR₂-AP on mice *in vivo*. Blood pressure data collected during the baseline period corresponds to previous work that indicated higher systolic blood pressures in PAR₂^{-/-} than C57 (McGuire *et al.*, 2008). The reasons for an increased baseline systolic blood pressure in PAR₂^{-/-} are attributed to the lack of PAR₂ and other phenotypic variations that may arise through development of these knockout mice. The anticipated hypotensive effect of PAR₂-AP that was reported in acute studies with rats and mice was observed during chronic 2fly treatment in our study, but the magnitude of effect that we observed was on a much smaller scale.

Previous studies in anaesthetized mice (Cheung *et al.*, 1998) and unrestrained rats via radio telemetry (Wang *et al.*, 2010) measured reductions of 10-40 mmHg and >60 mmHg respectively. In C57 we found 2fly HD lowered the mean systolic and pulse pressures by ~7 and ~4 mmHg, respectively, relative to the baseline period. The small lowering effect of 2fly *in vivo* may be partly explained by the apparent desensitization to PAR₂-AP of blood vessels. It would be expected that attenuated acetylcholine responses would be associated with higher blood pressures. In this model, it seems that the

endothelium dysfunction was small enough to be overridden by the hypotensive actions of 2fly. Nevertheless, a hypotensive effect *in vivo* of 2fly occurred despite the presence of endothelium dysfunction which suggests that PAR₂-induced hypotension in the absence of endothelial dysfunction (as would occur in an acute administered dose) may be of larger magnitude (Cheung *et al.*, 1998; Damiano *et al.*, 1999; Wang *et al.*, 2010).

5.4 Limitations to interpretations

There were some limitations in this study. The first limitation is the selection of blood vessel to measure. Data in resistance vasculature such as mesenteric arteries, along with aortas (a compliance vessel), would have added to the information that was obtained and allowed a more detailed description of any results obtained. Nevertheless the relaxation actions of PAR₂-AP on the aorta *in vitro* would be consistent with the isolated effect *in vivo* of PAR₂-AP on systolic arterial and pulse pressures. A second limitation to the interpretations is that all of the data was obtained in males and the effect of the treatment in females was not measured. We have no reason to suggest that females would react differently to treatment, but also have no data to prove that they do not. A third limitation is in measurement of protein expression. Although there is variability in individual groups the sample size is sufficient to be confident of the results. With regards to eNOS expression a measurement of phosphorylated eNOS compared with unphosphorylated eNOS may offer an alternative interpretation about the level of eNOS activity in the two treatment groups. A fourth limitation is we do not know the concentrations of 2fly in the blood and tissues that are achieved through this

subcutaneous route. It would help in our interpretation of the blood pressure changes in relation to acute studies that administered 2fly intravenously. Knowing the final concentration in blood would allow us to titrate subcutaneous 2fly to match intravenous administration to see if chronic administration at the same dose as in these studies would elicit the large drops in blood pressures measured acutely.

5.5 Conclusions

Chronic *in vivo* administered PAR₂-AP produced a dysfunction of vascular reactivity in mouse aortas, which was characterized by attenuated endothelium-dependent PAR₂ and cholinergic as well as endothelium-independent nitric oxide-mediated relaxations as expected by **Hypothesis 1** (but only at specific time and doses). The vascular dysfunction caused by high dose PAR₂-AP was accompanied by significant changes in blood pressures which supported **Hypothesis 2**.

To investigate the mechanisms underlying endothelium dysfunction of aortas in this model, it may be of interest to measure the levels of inflammatory molecules in each of the treatment groups. Inflammation is known to be associated with endothelial dysfunction, and thus, pro-inflammatory mediators e.g. cytokines, may play an integral part in the changes that occur in the attenuation of endothelium-dependent and -independent induced relaxations. This chronic PAR₂-AP infusion model represents an interesting approach to examining the possible connections between the activation of PAR₂ and the development of cardiovascular diseases involving vascular dysfunction.

References

- Ahn HS, Chackalamannil S, Boykow G, Graziano MP, Foster C. Development of proteinase-activated receptor 1 antagonists as therapeutic agents for thrombosis, restenosis and inflammatory diseases. *Curr Pharm Des* 2003;9(28):2349-2365.
- Al-Ani B, Saifeddine M, Hollenberg MD. Detection of functional receptors for the proteinase-activated-receptor-2-activating polypeptide, SLIGRL-NH₂, in rat vascular and gastric smooth muscle. *Can J Physiol Pharmacol* 1995 Aug;73(8):1203-1207.
- Al-Ani B, Saifeddine M, Kawabata A, Renaux B, Mokashi S, Hollenberg MD. Proteinase-activated receptor 2 (PAR(2)): development of a ligand-binding assay correlating with activation of PAR(2) by PAR(1)- and PAR(2)-derived peptide ligands. *J Pharmacol Exp Ther* 1999 Aug;290(2):753-760.
- Al-Ani B, Saifeddine M, Wijesuriya SJ, Hollenberg MD. Modified proteinase-activated receptor-1 and -2 derived peptides inhibit proteinase-activated receptor-2 activation by trypsin. *J Pharmacol Exp Ther* 2002 Feb;300(2):702-708.
- Anderson TJ, Uehata A, Gerhard MD, Meredith IT, Knab S, Delagrangé D, et al. Close relation of endothelial function in the human coronary and peripheral circulations. *J Am Coll Cardiol* 1995 Nov 1;26(5):1235-1241.
- Barry GD, Suen JY, Le GT, Cotterell A, Reid RC, Fairlie DP. Novel agonists and antagonists for human protease activated receptor 2. *J Med Chem* 2010 Oct 28;53(20):7428-7440.
- Brunner H, Cockcroft JR, Deanfield J, Donald A, Ferrannini E, Halcox J, et al. Endothelial function and dysfunction. Part II: Association with cardiovascular risk factors and diseases. A statement by the Working Group on Endothelins and Endothelial Factors of the European Society of Hypertension. *J Hypertens* 2005 Feb;23(2):233-246.
- Buddenkotte J, Stroh C, Engels IH, Moormann C, Shpacovitch VM, Seeliger S, et al. Agonists of proteinase-activated receptor-2 stimulate upregulation of intercellular cell adhesion molecule-1 in primary human keratinocytes via activation of NF-kappa B. *J Invest Dermatol* 2005 Jan;124(1):38-45.
- Cameron NE, Cotter MA. Impaired contraction and relaxation in aorta from streptozotocin-diabetic rats: role of polyol pathway. *Diabetologia* 1992 Nov;35(11):1011-1019.

- Celermajer DS, Sorensen KE, Gooch VM, Spiegelhalter DJ, Miller OI, Sullivan ID, et al. Non-invasive detection of endothelial dysfunction in children and adults at risk of atherosclerosis. *Lancet* 1992 Nov 7;340(8828):1111-1115.
- Cenac N, Coelho AM, Nguyen C, Compton S, Andrade-Gordon P, MacNaughton WK, et al. Induction of intestinal inflammation in mouse by activation of proteinase-activated receptor-2. *Am J Pathol* 2002 Nov;161(5):1903-1915.
- Chataigneau T, Feletou M, Huang PL, Fishman MC, Duhault J, Vanhoutte PM. Acetylcholine-induced relaxation in blood vessels from endothelial nitric oxide synthase knockout mice. *Br J Pharmacol* 1999 Jan;126(1):219-226.
- Cheung WM, Andrade-Gordon P, Derian CK, Damiano BP. Receptor-activating peptides distinguish thrombin receptor (PAR-1) and protease activated receptor 2 (PAR-2) mediated hemodynamic responses in vivo. *Can J Physiol Pharmacol* 1998 Jan;76(1):16-25.
- Connolly AJ, Ishihara H, Kahn ML, Farese RV, Jr, Coughlin SR. Role of the thrombin receptor in development and evidence for a second receptor. *Nature* 1996 Jun 6;381(6582):516-519.
- Covic L, Gresser AL, Talavera J, Swift S, Kuliopulos A. Activation and inhibition of G protein-coupled receptors by cell-penetrating membrane-tethered peptides. *Proc Natl Acad Sci U S A* 2002 Jan 22;99(2):643-648.
- Cox DA, Vita JA, Treasure CB, Fish RD, Alexander RW, Ganz P, et al. Atherosclerosis impairs flow-mediated dilation of coronary arteries in humans. *Circulation* 1989 Sep;80(3):458-465.
- Damiano BP, Cheung WM, Santulli RJ, Fung-Leung WP, Ngo K, Ye RD, et al. Cardiovascular responses mediated by protease-activated receptor-2 (PAR-2) and thrombin receptor (PAR-1) are distinguished in mice deficient in PAR-2 or PAR-1. *J Pharmacol Exp Ther* 1999 Feb;288(2):671-678.
- D'Andrea MR, Derian CK, Leturcq D, Baker SM, Brunmark A, Ling P, et al. Characterization of protease-activated receptor-2 immunoreactivity in normal human tissues. *J Histochem Cytochem* 1998 Feb;46(2):157-164.
- Dauphin F, Hamel E. Muscarinic receptor subtype mediating vasodilation feline middle cerebral artery exhibits M3 pharmacology. *Eur J Pharmacol* 1990 Mar 20;178(2):203-213.
- De Campo BA, Henry PJ. Stimulation of protease-activated receptor-2 inhibits airway eosinophilia, hyperresponsiveness and bronchoconstriction in a murine model of allergic inflammation. *Br J Pharmacol* 2005 Apr;144(8):1100-1108.

Deanfield J, Donald A, Ferri C, Giannattasio C, Halcox J, Halligan S, et al. Endothelial function and dysfunction. Part I: Methodological issues for assessment in the different vascular beds: a statement by the Working Group on Endothelin and Endothelial Factors of the European Society of Hypertension. *J Hypertens* 2005 Jan;23(1):7-17.

Dery O, Corvera CU, Steinhoff M, Bunnett NW. Proteinase-activated receptors: novel mechanisms of signaling by serine proteases. *Am J Physiol* 1998 Jun;274(6 Pt 1):C1429-52.

Dohi Y, Criscione L, Luscher TF. Renovascular hypertension impairs formation of endothelium-derived relaxing factors and sensitivity to endothelin-1 in resistance arteries. *Br J Pharmacol* 1991 Oct;104(2):349-354.

Emilsson K, Wahlestedt C, Sun MK, Nystedt S, Owman C, Sundelin J. Vascular effects of proteinase-activated receptor 2 agonist peptide. *J Vasc Res* 1997 Jul-Aug;34(4):267-272.

Endemann DH, Schiffrin EL. Endothelial dysfunction. *J Am Soc Nephrol* 2004 Aug;15(8):1983-1992.

Ferrell WR, Lockhart JC, Kelso EB, Dunning L, Plevin R, Meek SE, et al. Essential role for proteinase-activated receptor-2 in arthritis. *J Clin Invest* 2003 Jan;111(1):35-41.

Fiorucci S, Mencarelli A, Palazzetti B, Distrutti E, Vergnolle N, Hollenberg MD, et al. Proteinase-activated receptor 2 is an anti-inflammatory signal for colonic lamina propria lymphocytes in a mouse model of colitis. *Proc Natl Acad Sci U S A* 2001 Nov 20;98(24):13936-13941.

Furchgott RF. Role of endothelium in responses of vascular smooth muscle. *Circ Res* 1983 Nov;53(5):557-573.

Furchgott RF, Zawadzki JV. The obligatory role of endothelial cells in the relaxation of arterial smooth muscle by acetylcholine. *Nature* 1980 Nov 27;288(5789):373-376.

Goon Goh F, Sloss CM, Cunningham MR, Nilsson M, Cadalbert L, Plevin R. G-protein-dependent and -independent pathways regulate proteinase-activated receptor-2 mediated p65 NFkappaB serine 536 phosphorylation in human keratinocytes. *Cell Signal* 2008 Jul;20(7):1267-1274.

Hamilton JR, Moffatt JD, Tatoulis J, Cocks TM. Enzymatic activation of endothelial protease-activated receptors is dependent on artery diameter in human and porcine isolated coronary arteries. *Br J Pharmacol* 2002 Jun;136(4):492-501.

- Hansen KK, Oikonomopoulou K, Li Y, Hollenberg MD. Proteinases, proteinase-activated receptors (PARs) and the pathophysiology of cancer and diseases of the cardiovascular, musculoskeletal, nervous and gastrointestinal systems. *Naunyn Schmiedebergs Arch Pharmacol* 2008 Jun;377(4-6):377-392.
- Harrison DG. Cellular and molecular mechanisms of endothelial cell dysfunction. *J Clin Invest* 1997 Nov 1;100(9):2153-2157.
- Hollenberg MD. Proteinase-mediated signaling: proteinase-activated receptors (PARs) and much more. *Life Sci* 2003 Dec 5;74(2-3):237-246.
- Hollenberg MD, Saifeddine M, Al-Ani B, Gui Y. Proteinase-activated receptor 4 (PAR4): action of PAR4-activating peptides in vascular and gastric tissue and lack of cross-reactivity with PAR1 and PAR2. *Can J Physiol Pharmacol* 1999 Jun;77(6):458-464.
- Hollenberg MD, Saifeddine M, al-Ani B, Kawabata A. Proteinase-activated receptors: structural requirements for activity, receptor cross-reactivity, and receptor selectivity of receptor-activating peptides. *Can J Physiol Pharmacol* 1997 Jul;75(7):832-841.
- Ide J, Aoki T, Ishivata S, Glusa E, Strukova SM. Proteinase-activated receptor agonists stimulate the increase in intracellular Ca²⁺ in cardiomyocytes and proliferation of cardiac fibroblasts from chick embryos. *Bull Exp Biol Med* 2007 Dec;144(6):760-763.
- Ishihara H, Connolly AJ, Zeng D, Kahn ML, Zheng YW, Timmons C, et al. Protease-activated receptor 3 is a second thrombin receptor in humans. *Nature* 1997 Apr 3;386(6624):502-506.
- Jin G, Hayashi T, Kawagoe J, Takizawa T, Nagata T, Nagano I, et al. Deficiency of PAR-2 gene increases acute focal ischemic brain injury. *J Cereb Blood Flow Metab* 2005 Mar;25(3):302-313.
- Kagota S, Chia E, McGuire JJ. Preserved arterial vasodilation via endothelial protease-activated receptor-2 in obese type 2 diabetic mice. *Br J Pharmacol* 2011 Mar 22.
- Kahn ML, Zheng YW, Huang W, Bigornia V, Zeng D, Moff S, et al. A dual thrombin receptor system for platelet activation. *Nature* 1998 Aug 13;394(6694):690-694.
- Kaneider NC, Leger AJ, Agarwal A, Nguyen N, Perides G, Derian C, et al. 'Role reversal' for the receptor PAR1 in sepsis-induced vascular damage. *Nat Immunol* 2007 Dec;8(12):1303-1312.
- Kanke T, Kabeya M, Kubo S, Kondo S, Yasuoka K, Tagashira J, et al. Novel antagonists for proteinase-activated receptor 2: inhibition of cellular and vascular responses in vitro and in vivo. *Br J Pharmacol* 2009 Sep;158(1):361-371.

- Kanke T, Macfarlane SR, Seatter MJ, Davenport E, Paul A, McKenzie RC, et al. Proteinase-activated receptor-2-mediated activation of stress-activated protein kinases and inhibitory kappa B kinases in NCTC 2544 keratinocytes. *J Biol Chem* 2001 Aug 24;276(34):31657-31666.
- Kaufmann R, Oettel C, Horn A, Halbhuber KJ, Eitner A, Krieg R, et al. Met receptor tyrosine kinase transactivation is involved in proteinase-activated receptor-2-mediated hepatocellular carcinoma cell invasion. *Carcinogenesis* 2009 Sep;30(9):1487-1496.
- Kawabata A, Kanke T, Yonezawa D, Ishiki T, Saka M, Kabeya M, et al. Potent and metabolically stable agonists for protease-activated receptor-2: evaluation of activity in multiple assay systems in vitro and in vivo. *J Pharmacol Exp Ther* 2004 Jun;309(3):1098-1107.
- Kawabata A, Kuroda R, Minami T, Kataoka K, Taneda M. Increased vascular permeability by a specific agonist of protease-activated receptor-2 in rat hindpaw. *Br J Pharmacol* 1998 Oct;125(3):419-422.
- Kawabata A, Nishikawa H, Kuroda R, Kawai K, Hollenberg MD. Proteinase-activated receptor-2 (PAR-2): regulation of salivary and pancreatic exocrine secretion in vivo in rats and mice. *Br J Pharmacol* 2000 Apr;129(8):1808-1814.
- Kelso EB, Lockhart JC, Hembrough T, Dunning L, Plevin R, Hollenberg MD, et al. Therapeutic promise of proteinase-activated receptor-2 antagonism in joint inflammation. *J Pharmacol Exp Ther* 2006 Mar;316(3):1017-1024.
- Kwon NS, Nathan CF, Gilker C, Griffith OW, Matthews DE, Stuehr DJ. L-citrulline production from L-arginine by macrophage nitric oxide synthase. The ureido oxygen derives from dioxygen. *J Biol Chem* 1990 Aug 15;265(23):13442-13445.
- Lan RS, Knight DA, Stewart GA, Henry PJ. Role of PGE(2) in protease-activated receptor-1, -2 and -4 mediated relaxation in the mouse isolated trachea. *Br J Pharmacol* 2001 Jan;132(1):93-100.
- Laukkarinen JM, Weiss ER, van Acker GJ, Steer ML, Perides G. Protease-activated receptor-2 exerts contrasting model-specific effects on acute experimental pancreatitis. *J Biol Chem* 2008 Jul 25;283(30):20703-20712.
- Lindner JR, Kahn ML, Coughlin SR, Sambrano GR, Schauble E, Bernstein D, et al. Delayed onset of inflammation in protease-activated receptor-2-deficient mice. *J Immunol* 2000 Dec 1;165(11):6504-6510.

- Lourbakos A, Yuan YP, Jenkins AL, Travis J, Andrade-Gordon P, Santulli R, et al. Activation of protease-activated receptors by gingipains from *Porphyromonas gingivalis* leads to platelet aggregation: a new trait in microbial pathogenicity. *Blood* 2001 Jun 15;97(12):3790-3797.
- Luscher TF, Diederich D, Weber E, Vanhoutte PM, Buhler FR. Endothelium-dependent responses in carotid and renal arteries of normotensive and hypertensive rats. *Hypertension* 1988 Jun;11(6 Pt 2):573-578.
- Luscher TF, Yang Z, Diederich D, Buhler FR. Endothelium-dependent vascular responses: effect of hypertension and cyclosporin A. *Z Kardiol* 1989;78 Suppl 6:132-136.
- Macfarlane SR, Seatter MJ, Kanke T, Hunter GD, Plevin R. Proteinase-activated receptors. *Pharmacol Rev* 2001 Jun;53(2):245-282.
- Macfarlane SR, Sloss CM, Cameron P, Kanke T, McKenzie RC, Plevin R. The role of intracellular Ca²⁺ in the regulation of proteinase-activated receptor-2 mediated nuclear factor kappa B signalling in keratinocytes. *Br J Pharmacol* 2005 Jun;145(4):535-544.
- Matsubara M, Titani K, Taniguchi H. Interaction of calmodulin-binding domain peptides of nitric oxide synthase with membrane phospholipids: regulation by protein phosphorylation and Ca(2+)-calmodulin. *Biochemistry* 1996 Nov 19;35(46):14651-14658.
- McGuire JJ, Dai J, Andrade-Gordon P, Triggle CR, Hollenberg MD. Proteinase-activated receptor-2 (PAR2): vascular effects of a PAR2-derived activating peptide via a receptor different than PAR2. *J Pharmacol Exp Ther* 2002a Dec;303(3):985-992.
- McGuire JJ, Hollenberg MD, Andrade-Gordon P, Triggle CR. Multiple mechanisms of vascular smooth muscle relaxation by the activation of proteinase-activated receptor 2 in mouse mesenteric arterioles. *Br J Pharmacol* 2002b Jan;135(1):155-169.
- McGuire JJ, Hollenberg MD, Bennett BM, Triggle CR. Hyperpolarization of murine small caliber mesenteric arteries by activation of endothelial proteinase-activated receptor 2. *Can J Physiol Pharmacol* 2004a Dec;82(12):1103-1112.
- McGuire JJ, Saifeddine M, Triggle CR, Sun K, Hollenberg MD. 2-furoyl-LIGRLO-amide: a potent and selective proteinase-activated receptor 2 agonist. *J Pharmacol Exp Ther* 2004b Jun;309(3):1124-1131.
- McGuire JJ, Van Vliet BN, Gimenez J, King JC, Halfyard SJ. Persistence of PAR-2 vasodilation despite endothelial dysfunction in BPH/2 hypertensive mice. *Pflugers Arch* 2007 Jul;454(4):535-543.

McGuire JJ, Van Vliet BN, Halfyard SJ. Blood pressures, heart rate and locomotor activity during salt loading and angiotensin II infusion in protease-activated receptor 2 (PAR2) knockout mice. *BMC Physiol* 2008 Oct 21;8:20.

Mcguire JJ. Proteinase-Activated Receptor 2 (PAR2): A Challenging New Target for Treatment of Vascular Diseases. *Curr Pharm Des* 2004 08;10(22):2769-2778.

McLean PG, Aston D, Sarkar D, Ahluwalia A. Protease-activated receptor-2 activation causes EDHF-like coronary vasodilation: selective preservation in ischemia/reperfusion injury: involvement of lipoxigenase products, VR1 receptors, and C-fibers. *Circ Res* 2002 Mar 8;90(4):465-472.

Molino M, Barnathan ES, Numerof R, Clark J, Dreyer M, Cumashi A, et al. Interactions of mast cell tryptase with thrombin receptors and PAR-2. *J Biol Chem* 1997 Feb 14;272(7):4043-4049.

Mulvany MJ, Halpern W. Contractile properties of small arterial resistance vessels in spontaneously hypertensive and normotensive rats. *Circ Res* 1977 Jul;41(1):19-26.

Napoli C, Cicala C, Wallace JL, de Nigris F, Santagada V, Caliendo G, et al. Protease-activated receptor-2 modulates myocardial ischemia-reperfusion injury in the rat heart. *Proc Natl Acad Sci U S A* 2000 Mar 28;97(7):3678-3683.

Noh DY, Shin SH, Rhee SG. Phosphoinositide-specific phospholipase C and mitogenic signaling. *Biochim Biophys Acta* 1995 Dec 18;1242(2):99-113.

Nystedt S, Ramakrishnan V, Sundelin J. The proteinase-activated receptor 2 is induced by inflammatory mediators in human endothelial cells. Comparison with the thrombin receptor. *J Biol Chem* 1996 Jun 21;271(25):14910-14915.

Panza JA, Quyyumi AA, Brush JE, Jr, Epstein SE. Abnormal endothelium-dependent vascular relaxation in patients with essential hypertension. *N Engl J Med* 1990 Jul 5;323(1):22-27.

Perticone F, Ceravolo R, Pujia A, Ventura G, Iacopino S, Scozzafava A, et al. Prognostic significance of endothelial dysfunction in hypertensive patients. *Circulation* 2001 Jul 10;104(2):191-196.

Popescu LM, Panoiu C, Hinescu M, Nutu O. The mechanism of cGMP-induced relaxation in vascular smooth muscle. *Eur J Pharmacol* 1985 Jan 8;107(3):393-394.

Quyyumi AA, Mulcahy D, Andrews NP, Husain S, Panza JA, Cannon RO, 3rd. Coronary vascular nitric oxide activity in hypertension and hypercholesterolemia. Comparison of acetylcholine and substance P. *Circulation* 1997 Jan 7;95(1):104-110.

Rajagopalan S, Kurz S, Munzel T, Tarpey M, Freeman BA, Griending KK, et al. Angiotensin II-mediated hypertension in the rat increases vascular superoxide production via membrane NADH/NADPH oxidase activation. Contribution to alterations of vasomotor tone. *J Clin Invest* 1996 Apr 15;97(8):1916-1923.

Rao DN, Cederbaum AI. Production of nitric oxide and other iron-containing metabolites during the reductive metabolism of nitroprusside by microsomes and by thiols. *Arch Biochem Biophys* 1995 Aug 20;321(2):363-371.

Reed PW, Lardy HA. A23187: a divalent cation ionophore. *J Biol Chem* 1972 Nov 10;247(21):6970-6977.

Ritchie E, Saka M, Mackenzie C, Drummond R, Wheeler-Jones C, Kanke T, et al. Cytokine upregulation of proteinase-activated-receptors 2 and 4 expression mediated by p38 MAP kinase and inhibitory kappa B kinase beta in human endothelial cells. *Br J Pharmacol* 2007 Apr;150(8):1044-1054.

Robin J, Kharbanda R, Mclean P, Campbell R, Vallance P. Protease-activated receptor 2-mediated vasodilatation in humans in vivo: role of nitric oxide and prostanoids. *Circulation* 2003 Feb 25;107(7):954-959.

Sabri A, Guo J, Elouardighi H, Darrow AL, Andrade-Gordon P, Steinberg SF. Mechanisms of protease-activated receptor-4 actions in cardiomyocytes. Role of Src tyrosine kinase. *J Biol Chem* 2003 Mar 28;278(13):11714-11720.

Saifeddine M, al-Ani B, Cheng CH, Wang L, Hollenberg MD. Rat proteinase-activated receptor-2 (PAR-2): cDNA sequence and activity of receptor-derived peptides in gastric and vascular tissue. *Br J Pharmacol* 1996 Jun;118(3):521-530.

Schachinger V, Britten MB, Zeiher AM. Prognostic impact of coronary vasodilator dysfunction on adverse long-term outcome of coronary heart disease. *Circulation* 2000 Apr 25;101(16):1899-1906.

Schachinger V, Zeiher AM. Quantitative assessment of coronary vasoreactivity in humans in vivo. Importance of baseline vasomotor tone in atherosclerosis. *Circulation* 1995 Oct 15;92(8):2087-2094.

Schindler TH, Nitzsche EU, Munzel T, Olschewski M, Brink I, Jeserich M, et al. Coronary vasoregulation in patients with various risk factors in response to cold pressor testing: contrasting myocardial blood flow responses to short- and long-term vitamin C administration. *J Am Coll Cardiol* 2003 Sep 3;42(5):814-822.

Schmidlin F, Amadesi S, Dabbagh K, Lewis DE, Knott P, Bunnett NW, et al. Protease-activated receptor 2 mediates eosinophil infiltration and hyperreactivity in allergic inflammation of the airway. *J Immunol* 2002 Nov 1;169(9):5315-5321.

- Seeliger S, Derian CK, Vergnolle N, Bunnett NW, Nawroth R, Schmelz M, et al. Proinflammatory role of proteinase-activated receptor-2 in humans and mice during cutaneous inflammation in vivo. *FASEB J* 2003 Oct;17(13):1871-1885.
- Sharma A, Tao X, Gopal A, Ligon B, Andrade-Gordon P, Steer ML, et al. Protection against acute pancreatitis by activation of protease-activated receptor-2. *Am J Physiol Gastrointest Liver Physiol* 2005 Feb;288(2):G388-95.
- Shimada SG, Shimada KA, Collins JG. Scratching behavior in mice induced by the proteinase-activated receptor-2 agonist, SLIGRL-NH₂. *Eur J Pharmacol* 2006 Jan 20;530(3):281-283.
- Shpacovitch VM, Varga G, Strey A, Gunzer M, Mooren F, Buddenkotte J, et al. Agonists of proteinase-activated receptor-2 modulate human neutrophil cytokine secretion, expression of cell adhesion molecules, and migration within 3-D collagen lattices. *J Leukoc Biol* 2004 Aug;76(2):388-398.
- Smeda JS, McGuire JJ. Effects of poststroke losartan versus captopril treatment on myogenic and endothelial function in the cerebrovasculature of SHRsp. *Stroke* 2007 May;38(5):1590-1596.
- Smeda JS, McGuire JJ, Daneshtalab N. Protease-activated receptor 2 and bradykinin-mediated vasodilation in the cerebral arteries of stroke-prone rats. *Peptides* 2010 Feb;31(2):227-237.
- Sobey CG, Moffatt JD, Cocks TM. Evidence for selective effects of chronic hypertension on cerebral artery vasodilatation to protease-activated receptor-2 activation. *Stroke* 1999 Sep;30(9):1933-40; discussion 1941.
- SoRelle R. Nobel prize awarded to scientists for nitric oxide discoveries. *Circulation* 1998 Dec 1;98(22):2365-2366.
- Statistics Canada, CANSIM Table 102-0529: Deaths, by cause, Chapter IX: Diseases of the circulatory system (I00 to I99), age group and sex, Canada, annual (number), 2000 to 2006. Released May 4, 2010.
- Stull JT, Hsu LC, Tansey MG, Kamm KE. Myosin light chain kinase phosphorylation in tracheal smooth muscle. *J Biol Chem* 1990 Sep 25;265(27):16683-16690.
- Tansey MG, Word RA, Hidaka H, Singer HA, Schworer CM, Kamm KE, et al. Phosphorylation of myosin light chain kinase by the multifunctional calmodulin-dependent protein kinase II in smooth muscle cells. *J Biol Chem* 1992 Jun 25;267(18):12511-12516.
- Tesfamariam B, Jakubowski JA, Cohen RA. Contraction of diabetic rabbit aorta caused by endothelium-derived PGH₂-TxA₂. *Am J Physiol* 1989 Nov;257(5 Pt 2):H1327-33.

Twort CH, van Breemen C. Cyclic guanosine monophosphate-enhanced sequestration of Ca²⁺ by sarcoplasmic reticulum in vascular smooth muscle. *Circ Res* 1988 May;62(5):961-964.

Urbich C, Dimmeler S. CD40 and vascular inflammation. *Can J Cardiol* 2004 May 15;20(7):681-683.

Van Vliet BN, McGuire J, Chafe L, Leonard A, Joshi A, Montani JP. Phenotyping the level of blood pressure by telemetry in mice. *Clin Exp Pharmacol Physiol* 2006 Nov;33(11):1007-1015.

Vancheri C, Mastruzzo C, Sortino MA, Crimi N. The lung as a privileged site for the beneficial actions of PGE₂. *Trends Immunol* 2004 Jan;25(1):40-46.

Vergnolle N, Bunnett NW, Sharkey KA, Brussee V, Compton SJ, Grady EF, et al. Proteinase-activated receptor-2 and hyperalgesia: A novel pain pathway. *Nat Med* 2001 Jul;7(7):821-826.

Vergnolle N, Hollenberg MD, Sharkey KA, Wallace JL. Characterization of the inflammatory response to proteinase-activated receptor-2 (PAR₂)-activating peptides in the rat paw. *Br J Pharmacol* 1999 Jul;127(5):1083-1090.

Virdis A, Iglarz M, Neves MF, Amiri F, Touyz RM, Rozen R, et al. Effect of hyperhomocystinemia and hypertension on endothelial function in methylenetetrahydrofolate reductase-deficient mice. *Arterioscler Thromb Vasc Biol* 2003 Aug 1;23(8):1352-1357.

Volpe M, Iaccarino G, Vecchione C, Rizzoni D, Russo R, Rubattu S, et al. Association and cosegregation of stroke with impaired endothelium-dependent vasorelaxation in stroke prone, spontaneously hypertensive rats. *J Clin Invest* 1996 Jul 15;98(2):256-261.

Vu TK, Hung DT, Wheaton VI, Coughlin SR. Molecular cloning of a functional thrombin receptor reveals a novel proteolytic mechanism of receptor activation. *Cell* 1991 Mar 22;64(6):1057-1068.

Wang J, Boerma M, Kulkarni A, Hollenberg MD, Hauer-Jensen M. Activation of protease activated receptor 2 by exogenous agonist exacerbates early radiation injury in rat intestine. *Int J Radiat Oncol Biol Phys* 2010 Jul 15;77(4):1206-1212.

Wanstall JC, Gambino A. Proteinase-activated receptor (PAR)-mediated vasorelaxation in pulmonary arteries from normotensive and hypoxic pulmonary hypertensive rats. *Pulm Pharmacol Ther* 2004;17(2):97-103.

Yoshida N, Katada K, Handa O, Takagi T, Kokura S, Naito Y, et al. Interleukin-8 production via protease-activated receptor 2 in human esophageal epithelial cells. *Int J Mol Med* 2007 Feb;19(2):335-340.

Appendix A

#	Primer	Sequence (5' to 3')	T _m (°C)
1	IMR5332 (Mutant)	GCCAGAGGCCACTTGTGTAG	64.5
2	IMR7419 (Forward)	TCAAAGACTGCTGGTGGTTG	60.4
3	IMR7420 (Reverse)	GGTCCAACAGTAAGGCTGCT	62.5

Oligonucleotide primer sets for genotyping PAR₂ -/- mice. Product

from (1) and (2) = 198 bp → mutant → neomycin gene present

Product from (2) and (3) = 345 bp → wildtype → *mPAR2 Exon 2 present*

T_m represents the melting temperature for the oligonucleotides.

Appendix B

Antibody	Relative molecular weight (kDa)	Reactivity	Catalogue #	Supplier	Dilution
rabbit anti-mouse, COX-1	70	mouse, Rat	160109	Cayman	1:800
goat anti-mouse, COX-2	70	mouse, rat, human	sc-1745	Santa Cruz	1:1000
rabbit anti-mouse, GAPDH-FL	37	mouse, rat, human	sc-25778	Santa Cruz	1:1000
goat anti-rabbit IgG HRP linked			10004301	Cayman	1:10000
donkey anti-goat IgG HRP linked			sc-2020	Santa Cruz	1:5000
rabbit anti-sGC	69	mouse	ab50333-100	Abcam	1:7500
mouse anti-eNOS	140	mouse, rat, human	610296	BD Transduction Lab.	1:7500
goat anti-rabbit IgG HRP linked			PI-1000	Vector	1:10000
horse anti-mouse IgG HRP linked			PI2000	Vector	1:10000

Antibodies used in western blot analysis. HRP, horseradish peroxidase.

